

# ANALYSIS OF THE DIFFUSE INTERFACE METHOD FOR THE STOKES-DARCY COUPLED PROBLEM

MARTINA BUKAČ\* AND BORIS MUHA†

**Abstract.** We consider the interaction between a free flowing fluid and a porous medium flow, where the free flowing fluid is described using the time dependent Stokes equations, and the porous medium flow is described using Darcy’s law in the primal formulation. To solve this problem numerically, we use the diffuse interface approach, where the weak form of the coupled problem is written on an extended domain which contains both Stokes and Darcy regions. This is achieved using a phase-field function which equals one in the Stokes region and zero in the Darcy region, and smoothly transitions between these two values on a diffuse region of width  $\epsilon$  around the Stokes-Darcy interface. We prove the convergence of the diffuse interface formulation to the standard, sharp interface formulation, and derive the rates of the convergence. This is performed by analyzing the modeling error of the diffuse interface approach at the continuous level, and by deriving the a priori error estimates for the diffuse interface method at the discrete level. The convergence rates are also derived computationally in a numerical example.

**Key words.** Stokes-Darcy; diffuse interface method; error analysis; rate of convergence

**AMS subject classifications.** 65M12, 65M15

**1. Introduction.** The interaction between a free flowing fluid and a porous medium flow, commonly formulated as a Stokes-Darcy coupled system, has been used to describe problems arising in many applications, including environmental sciences, hydrology, petroleum engineering and biomedical engineering. Hence, the development of numerical methods for Stokes-Darcy problems has been an active area of research. Most existing numerical methods are based on a sharp interface approach, in the sense that the interface between the Stokes and Darcy regions is parametrized using an exact specification of its geometry and location, and the nodes in the computational mesh align with the interface. They include both monolithic and partitioned numerical methods. Some of the recently developed monolithic schemes include a two-grid method with backtracking for the stationary monolithic Stokes-Darcy problem proposed in [1] and a mortar multiscale finite element method presented in [2]. We also mention the work in [3, 4] based on the Nitsche’s penalty method. Non-iterative partitioned schemes based on various time-discretization strategies were developed in [5–10]. A third-order in time implicit-explicit algorithm based on the combination of the Adams–Moulton and the Adams–Bashforth scheme was proposed in [11], and iterative domain decomposition methods based on generalized Robin coupling conditions were derived in [12, 13].

While the sharp interface methods are widely used, the explicit interface parametrization may be difficult to obtain in case of complex geometries. The exact location is sometimes not known exactly or the geometry is complicated, making a proper approximation of the integrals error-prone and difficult to automate. This often occurs when geometries are obtained implicitly using imaging data, commonly used in patient-specific biomedical simulations. Hence, as one alternative to sharp interface approaches, diffuse interface methods have been introduced [14–20]. They are also known as the phase-field or the diffuse domain methods. While they have features in common with the level set method [21–24], they are fundamentally different since the level set method tracks the exact sharp interface without introducing any diffuse layers [20]. Other conceptually similar approaches include the fictitious domain method with a spread interface [25, 26], the immersed boundary method with interface forcing functions based on Dirac distributions [27, 28] and the fat boundary method [29, 30], among others. The diffuse interface method received strong attention from the applications point of view [31–41], however, many difficult questions remain to be theoretically addressed both at the continuous and the discrete level. One of the fundamental mathematical questions, whether the diffuse interface converges to a sharp interface when the width of the diffuse interface tends to zero, remains an open problem for many phase-field models.

Theoretically, the diffuse interface approach has been widely studied for elliptic problems and two-phase

---

\*Department of Applied and Computational Mathematics and Statistics, University of Notre Dame, South Bend, IN 46556, USA. Email: mbukac@nd.edu. (Corresponding author.) Partially supported by the National Science Foundation under grants DMS 1912908 and DCSD 1934300.

†Department of Mathematics, Faculty of Science, University of Zagreb, Croatia. Email: borism@math.hr. Partially supported by the Croatian Science Foundation (Hrvatska Zaklada za Znanost) grant number IP-2018-01-3706.

flow problems. Analysis of the diffuse interface method for elliptic problems has been studied in [16, 18, 42–44]. An elliptic problem was also considered in [45], where diffuse formulations of Nitsche’s method for imposing Dirichlet boundary conditions on phase-field approximations of sharp domains were studied. A Cahn-Larche phase-field model approximating an elasticity sharp interface problem has been considered in [46]. Advection–diffusion on evolving diffuse interfaces has been studied in [32, 33]. We also mention the work in [47] where the interaction between the two-phase free flow and two-phase porous media flow was considered, but the diffuse interface method was used to separate different phases in each region, while the Stokes-Darcy interface was captured by a mesh aligned with the interface and the two problems were decoupled using a classical approach. Diffuse interface models for two-phase flows have been extensively analyzed, see, e.g., [48–54]. However, only recently a rigorous sharp interface limit convergence result with convergence rates in strong norms has been proved [55]. The main challenges in the analysis of the diffuse interface problems involve proving the convergence of the diffuse interface to the sharp interface, and the estimation of the modeling error, which can be quite difficult to analyze and remains open for many problems

We consider the fluid–porous medium interaction described by the time–dependent Stokes–Darcy coupled problem. We discretize the problem in time using the backward Euler method, and in space using the finite element method. The focus of this paper is the convergence analysis of the diffuse interface to the sharp interface as the width of the diffuse layer goes to zero. This is performed in two steps. First, we derive the error estimates and prove the convergence for the finite element approximation of the diffuse interface method. Then, we analyze the convergence of the continuous diffuse interface formulation to the continuous sharp interface formulation, obtaining the convergence rates with respect to the width of the diffuse layer. The rates of convergence are also computed numerically.

The rest of this paper is organized as follows. Section 2 presents the mathematical model and introduces a diffuse interface formulation. We also prove that the problem is well-posed, and discretize the problem in time and space. The error analysis of the discrete diffuse interface problem is performed in Section 3, and the analysis of the modeling error is performed in Section 4. Numerical examples are presented in Section 5, and conclusions are drawn in Section 6.

## 2. The mathematical model.

**2.1. The sharp interface model.** Let  $\Omega_F$  denote the fluid domain and  $\Omega_D$  denote the porous medium domain. We assume that  $\Omega_F, \Omega_D \subset \mathbb{R}^d, d = 2, 3$  are open, smooth sets of the same dimension, and that the fluid–porous medium interface  $\Gamma$  is the common boundary between the two domains, i.e.  $\partial\Omega_F \cap \partial\Omega_D = \emptyset, \partial\bar{\Omega}_F \cap \partial\bar{\Omega}_D = \Gamma$ . To model the fluid flow, we use the time–dependent Stokes equations, given as follows:

$$(2.1) \quad \rho \partial_t \mathbf{u} = \nabla \cdot \boldsymbol{\sigma}(\nabla \mathbf{u}, \pi) + \mathbf{F} \quad \text{in } \Omega_F,$$

$$(2.2) \quad \nabla \cdot \mathbf{u} = 0 \quad \text{in } \Omega_F,$$

where  $\mathbf{u}$  is the fluid velocity,  $\rho$  is the fluid density,  $\boldsymbol{\sigma}(\mathbf{u}, \pi) = 2\nu \mathbf{D}(\mathbf{u}) - \pi \mathbb{I}$  is the fluid Cauchy stress tensor,  $\nu$  is the fluid viscosity,  $\pi$  denotes the pressure and  $\mathbf{F}$  is the density of volume force.

The porous medium flow is governed by Darcy’s law, written in the primal formulation as:

$$(2.3) \quad c_0 \partial_t p - \nabla \cdot (\boldsymbol{\kappa} \nabla p) = g \quad \text{in } \Omega_D,$$

where  $p$  is the Darcy pressure,  $c_0$  is the storativity and  $\boldsymbol{\kappa}$  is the hydraulic conductivity tensor. We assume that  $\boldsymbol{\kappa}$  is uniformly bounded and positive definite, so that  $0 < k_* \leq \lambda \leq k^*$ , where  $\lambda \in \lambda(\boldsymbol{\kappa})$ , and  $\lambda(\boldsymbol{\kappa})$  is the spectrum of  $\boldsymbol{\kappa}$ . We note that the porous medium flow can be computed from  $p$  as  $\mathbf{q} = -\boldsymbol{\kappa} \nabla p$ .

**Coupling conditions:** The Stokes and Darcy problems are coupled using the following interface conditions:

- The conservation of the mass:

$$\mathbf{u} \cdot \mathbf{n} = -\boldsymbol{\kappa} \nabla p \cdot \mathbf{n} \quad \text{on } \Gamma \times (0, T),$$

where  $\mathbf{n}$  is the unit normal to the fluid domain boundary.

- The Beavers-Joseph-Saffman condition:

$$\alpha_{BJ} \mathbf{u} \cdot \boldsymbol{\tau}_i + \boldsymbol{\sigma}(\mathbf{u}, \pi) \mathbf{n} \cdot \boldsymbol{\tau}_i = 0, \quad i = 1, 2, \dots, d-1, \quad \text{on } \Gamma \times (0, T),$$

where  $\boldsymbol{\tau}_i, i = 1, \dots, d-1$ , is the orthonormal basis for the tangential space of  $\Gamma$  and  $\alpha_{BJ}$  is the Beavers-Joseph-Saffman-Jones coefficient.

- The balance of pressure:

$$-\boldsymbol{\sigma}(\mathbf{u}, \pi) \mathbf{n} \cdot \mathbf{n} = p \text{ on } \Gamma \times (0, T).$$

**Boundary conditions:** We split the boundaries as:  $\partial\Omega_F = \Gamma \cup \Gamma_F^1 \cup \Gamma_F^2$ ,  $\partial\Omega_D = \Gamma \cup \Gamma_D^1 \cup \Gamma_D^2$ , and prescribe the following boundary conditions:

$$\begin{aligned} \mathbf{u} &= 0 & \text{on } \Gamma_F^1, \\ \boldsymbol{\sigma} \mathbf{n} &= 0 & \text{on } \Gamma_F^2, \\ p &= 0 & \text{on } \Gamma_D^1, \\ \partial_n p &= 0 & \text{on } \Gamma_D^2. \end{aligned}$$

REMARK 2.1. *In this paper, for simplicity, we consider only homogeneous boundary conditions. However, inhomogeneous boundary conditions can be easily included in the analysis by using the appropriate extension operators to homogenize the boundary conditions.*

**2.1.1. Weak formulation.** Given an open set  $S$ , we consider the usual Sobolev spaces  $H^k(S)$ , with  $k \geq 0$ . We introduce the following functional spaces:

$$\begin{aligned} \mathcal{V} &= \{\mathbf{u} \in (H^1(\Omega_F))^d : \mathbf{u} = 0 \text{ on } \Gamma_F^1\}, \\ \mathcal{X} &= \{\psi \in H^1(\Omega_D) : \psi = 0 \text{ on } \Gamma_D^1\}. \end{aligned}$$

The weak solution to the sharp interface Stokes-Darcy problem is defined as follows.

DEFINITION 2.1 (Weak solution of the sharp interface form). *We say that  $(\mathbf{u}, p, \pi) \in L^2(0, T; \mathcal{V} \times \mathcal{X}) \times H^{-1}(0, T; L^2(\Omega_F))$  is a weak solution if, for every  $(\mathbf{v}, \psi, \varphi) \in \mathcal{V} \times \mathcal{X} \times L^2(\Omega_F)$ , the following equality is satisfied in  $\mathcal{D}'(0, T)$ :*

$$\begin{aligned} \frac{d}{dt} \left( \int_{\Omega_F} \rho \mathbf{u} \cdot \mathbf{v} + c_0 \int_{\Omega_D} p \psi \right) + 2\nu \int_{\Omega_F} \mathbf{D}(\mathbf{u}) : \mathbf{D}(\mathbf{v}) + \int_{\Omega_D} \boldsymbol{\kappa} \nabla p \cdot \nabla \psi - \int_{\Omega_F} (\nabla \cdot \mathbf{v}) \pi + \int_{\Omega_F} (\nabla \cdot \mathbf{u}) \varphi \\ - \int_{\Gamma} \psi \mathbf{u} \cdot \mathbf{n} + \int_{\Gamma} p \mathbf{v} \cdot \mathbf{n} + \alpha_{BJ} \sum_{i=1}^{d-1} \int_{\Gamma} (\mathbf{u} \cdot \boldsymbol{\tau}_i) (\mathbf{v} \cdot \boldsymbol{\tau}_i) = \int_{\Omega_F} \mathbf{F} \cdot \mathbf{v} + \int_{\Omega_D} g \psi. \end{aligned}$$

Here,  $\mathcal{D}'(0, T)$  denotes the standard space of distributions on  $(0, T)$ . The weak solution satisfies the following energy equality:

$$\frac{1}{2} \frac{d}{dt} \left( \rho \|\mathbf{u}\|_{L^2(\Omega_F)}^2 + c_0 \|p\|_{L^2(\Omega_D)}^2 \right) + 2\nu \|\mathbf{D}(\mathbf{u})\|_{L^2(\Omega_F)}^2 + \alpha_{BJ} \sum_{i=1}^{d-1} \|\mathbf{u} \cdot \boldsymbol{\tau}_i\|_{L^2(\Gamma)}^2 + \|\boldsymbol{\kappa}^{\frac{1}{2}} \nabla p\|_{L^2(\Omega_D)}^2 = 0.$$

The theory of weak solutions for the Stokes-Darcy system is by now well understood, see, e.g., [56] for the stationary case and [57] for the evolution case.

**2.2. The diffuse interface formulation.** Denote by  $\chi$  the Heaviside function which equals one in  $\Omega_F$  and zero in  $\Omega_D$ . Let a phase field function  $\Phi^\epsilon : \Omega \rightarrow [0, 1]$  be a regularization of the Heaviside function such that  $\Phi^\epsilon \approx 1$  in  $\Omega_F$  and  $\Phi^\epsilon \approx 0$  in  $\Omega_D$ , and  $\Phi^\epsilon$  transitions between these two values on a “diffuse” layer of width  $\epsilon$ . We suppose that  $d\Gamma \approx |\nabla \Phi^\epsilon| dx$  and  $\mathbf{n} \approx -\frac{\nabla \Phi^\epsilon}{|\nabla \Phi^\epsilon|}$ . More precisely, we assume that the phase field function satisfies conditions from [18] (see Section 3, conditions (S1)-(S3)). An example of such function is  $\Phi^\epsilon(x) = \frac{1}{2} \left( 1 + S \left( \frac{d(X, \Gamma)}{\epsilon} \right) \right)$ , where  $d(\cdot, \Gamma)$  is a signed distance function, and

$$S(t) = \begin{cases} t, & t \leq 1, \\ \frac{t}{|t|}, & t > 1. \end{cases}$$

Then, we can write:

$$\begin{aligned}\int_{\Omega_F} F d\Omega &= \int_{\Omega} F \chi d\Omega \approx \int_{\Omega} F \Phi^\epsilon d\Omega, \\ \int_{\Omega_D} F d\Omega &= \int_{\Omega} F(1 - \chi) d\Omega \approx \int_{\Omega} F(1 - \Phi^\epsilon) d\Omega, \\ \int_{\Gamma} f d\Gamma &= \int_{\Omega} f \delta_\Gamma d\Omega \approx \int_{\Omega} f |\nabla \Phi^\epsilon| d\Omega,\end{aligned}$$

where  $\delta_\Gamma$  is a Dirac distribution at the interface  $\Gamma$ . Using the approximations above, and  $\mathbf{n} \approx -\frac{\nabla \Phi^\epsilon}{|\nabla \Phi^\epsilon|}$ , we can approximate the interface integrals as:

$$\int_{\Gamma} \psi \mathbf{u} \cdot \mathbf{n} \approx - \int_{\Omega} \psi \mathbf{u} \cdot \nabla \Phi^\epsilon, \quad \int_{\Gamma} p \mathbf{v} \cdot \mathbf{n} \approx - \int_{\Omega} p \mathbf{v} \cdot \nabla \Phi^\epsilon$$

and

$$\alpha_{BJ} \sum_{i=1}^{d-1} \int_{\Gamma} (\mathbf{u} \cdot \boldsymbol{\tau}_i)(\mathbf{v} \cdot \boldsymbol{\tau}_i) \approx \alpha_{BJ} \sum_{i=1}^{d-1} \int_{\Omega} (\mathbf{u} \cdot \tilde{\boldsymbol{\tau}}_i)(\mathbf{v} \cdot \tilde{\boldsymbol{\tau}}_i) |\nabla \Phi^\epsilon|,$$

where the tangent vectors  $\tilde{\boldsymbol{\tau}}_i$  are obtained directly from the phase-field function using the algorithm described in [31, 58]. We introduce the following regularization of  $\Phi^\epsilon$ :

$$(2.4) \quad \Phi^\epsilon = (1 - 2\delta)\Phi^\epsilon + \delta,$$

where  $\delta$  is a small positive number. Therefore,  $\Phi^\epsilon \geq \delta$  and  $1 - \Phi^\epsilon \geq \delta$ . Since we will keep  $\delta$  fixed throughout the next two sections, we do not write explicitly dependence of  $\Phi^\epsilon$  on  $\delta$ .

Every weight,  $\omega$ , induces a measure with density  $\omega dx$ , over the Borel sets of  $\mathbb{R}^n$ . For simplicity, this measure will also be denoted by  $\omega$ . For a Borel set  $E$ , we let  $\omega(E) = \int_E \omega dx$ . Similar as in [18], we define the weighted  $L^p$ -space associated to the measure  $\omega$  by:

$$L^p(\Omega, \omega) = \{ \psi : \Omega \rightarrow \mathbb{R} : |\psi|^p \omega \in L^1(\Omega) \},$$

with norm

$$\|\psi\|_{L^p(\Omega, \omega)}^p = \int_{\Omega} |\psi|^p \omega dx.$$

Associated with weighted  $L^p$ -spaces, we define the weighted Sobolev spaces:

$$H^k(\Omega, \omega) = \{ \psi \in L^2(\Omega, \omega) : D^\alpha \psi \in L^2(\Omega, \omega), \forall |\alpha| \leq k \},$$

with the corresponding norm

$$\|\phi\|_{H^k(\Omega, \omega)}^2 = \sum_{|\alpha| \leq k} \|D^\alpha \psi\|_{L^2(\Omega, \omega)}^2.$$

Notice that due to the regularization (2.4), the weighted spaces with weight  $\Phi^\epsilon$  are the same as the classical spaces as shown in the following lemma:

LEMMA 2.2. *For  $\delta > 0$ , we have  $L^2(\Omega) = L^2(\Omega, \Phi^\epsilon)$ , with equivalent norms given by:*

$$\sqrt{\delta} \|f\|_{L^2(\Omega)} \leq \|f\|_{L^2(\Omega, \Phi^\epsilon)} \leq \|f\|_{L^2(\Omega)}.$$

*Similarly,  $H^1(\Omega) = H^1(\Omega, \Phi^\epsilon)$ , with equivalent norms given by:*

$$\sqrt{\delta} \|f\|_{H^1(\Omega)} \leq \|f\|_{H^1(\Omega, \Phi^\epsilon)} \leq \|f\|_{H^1(\Omega)}.$$

*Proof.* Notice that, due to the regularization (2.4), the phase field function is bounded as  $\delta \leq \Phi^\epsilon \leq 1$ . Therefore, we have:

$$\|f\|_{L^2(\Omega)}^2 = \int_{\Omega} f^2 \leq \frac{1}{\delta} \int_{\Omega} \Phi^\epsilon f^2 = \frac{1}{\delta} \|f\|_{L^2(\Omega, \Phi^\epsilon)}^2,$$

$$\|f\|_{L^2(\Omega, \Phi^\epsilon)}^2 = \int_{\Omega} \Phi^\epsilon f^2 \leq \int_{\Omega} f^2 = \|f\|_{L^2(\Omega)}^2. \quad \square$$

Because in the phase field formulation all unknowns are defined on the whole domain,  $\Omega$ , we define the following Hilbert spaces for  $k \in \mathbb{N}$ :

$$\begin{aligned} \mathcal{V}^{k,\epsilon} &= \{\mathbf{u} \in (H^k(\Omega, \Phi^\epsilon))^d : \mathbf{u} = 0 \text{ on } \Gamma_F^1\}, & \mathcal{V}^\epsilon &= \mathcal{V}^{1,\epsilon}. \\ \mathcal{X}^{k,\epsilon} &= \{\psi \in H^k(\Omega, 1 - \Phi^\epsilon) : \psi = 0 \text{ on } \Gamma_D^1\}, & \mathcal{X}^\epsilon &= \mathcal{X}^{1,\epsilon}. \end{aligned}$$

Space  $\mathcal{V}^\epsilon$  is associated with the fluid velocity, while space  $\mathcal{X}^\epsilon$  is associated with the porous pressure. The following results from [18] and [59] will be used.

**LEMMA 2.3** (Trace inequality). *Let  $\epsilon_0$  be sufficiently small. Then, there exists a constant  $C_T > 0$  such that for  $0 < \epsilon < \epsilon_0$  and for  $\mathbf{v} \in W^{1,p}(\Omega, \Phi^\epsilon)$ ,  $1 \leq p \leq \infty$ , we have:*

$$\int_{\Omega} |\mathbf{v}|^p |\nabla \Phi^\epsilon| \leq C_T \|\mathbf{v}\|_{W^{1,p}(\Omega, \Phi^\epsilon)}^p.$$

**LEMMA 2.4** (Poincaré inequality). *We define  $W_0^{1,p}(\Omega, \Phi^\epsilon)$  as the closure of  $C_0^\infty(\Omega)$  in  $W^{1,p}(\Omega, \Phi^\epsilon)$  and set  $H_0^1(\Omega, \Phi^\epsilon) = W_0^{1,2}(\Omega, \Phi^\epsilon)$ . On these spaces, the following Poincaré inequality holds:*

$$\|\mathbf{v}\|_{L^p(\Omega, \Phi^\epsilon)} \leq C_P \|\nabla \mathbf{v}\|_{L^p(\Omega, \Phi^\epsilon)}, \quad \forall \mathbf{v} \in W_0^{1,p}(\Omega, \Phi^\epsilon),$$

where  $C_P$  depends on the diameter of  $\Omega$ , but is independent of  $\mathbf{v}$ .

**DEFINITION 2.5** (Weak solution of the diffuse interface form). *We say that  $(\mathbf{u}^\epsilon, p^\epsilon, \pi^\epsilon) \in L^2(0, T; \mathcal{V}^\epsilon \times \mathcal{X}^\epsilon) \times H^{-1}(0, T; L^2(\Omega))$  is a weak solution if, for every  $(\mathbf{v}, \psi, \varphi) \in \mathcal{V}^\epsilon \times \mathcal{X}^\epsilon \times L^2(\Omega)$ , the following equality is satisfied in  $\mathcal{D}'(0, T)$ :*

$$\begin{aligned} (2.5) \quad & \frac{d}{dt} \left( \int_{\Omega} \rho \mathbf{u}^\epsilon \cdot \mathbf{v} \Phi^\epsilon + c_0 \int_{\Omega} p^\epsilon \psi (1 - \Phi^\epsilon) \right) + 2\nu \int_{\Omega} \mathbf{D}(\mathbf{u}^\epsilon) : \mathbf{D}(\mathbf{v}) \Phi^\epsilon + \int_{\Omega} \kappa \nabla p^\epsilon \cdot \nabla \psi (1 - \Phi^\epsilon) \\ & - \int_{\Omega} (\nabla \cdot \mathbf{v}^\epsilon) \pi \Phi^\epsilon + \int_{\Omega} (\nabla \cdot \mathbf{u}^\epsilon) \varphi \Phi^\epsilon + \int_{\Omega} \psi \mathbf{u}^\epsilon \cdot \nabla \Phi^\epsilon - \int_{\Omega} p^\epsilon \mathbf{v} \cdot \nabla \Phi^\epsilon \\ & + \alpha_{BJ} \sum_{i=1}^{d-1} \int_{\Omega} (\mathbf{u} \cdot \tilde{\tau}_i) (\mathbf{v} \cdot \tilde{\tau}_i) |\nabla \Phi^\epsilon| = \int_{\Omega} \mathbf{F} \cdot \mathbf{v} \Phi^\epsilon + \int_{\Omega} g \psi (1 - \Phi^\epsilon). \end{aligned}$$

The goal of this paper is to analyze the convergence of the discrete phase field formulation of the Stokes-Darcy system to the solution of the continuous sharp interface problem. This will be done in two steps. In the first step, in Section 3, we fix  $\epsilon, \delta$  and the phase field function, and prove the error estimates for the finite element approximation of the diffuse interface formulation (2.5). In the second step, in Section 4, we analyze the convergence of the continuous diffuse interface formulation to the continuous sharp interface formulation.

Since in this section and Section 3 parameter  $\epsilon$  is fixed, we will omit writing superscript  $\epsilon$  in the unknowns for simplicity of notation. We start by proving the well-posedness for the phase field formulation.

**THEOREM 2.6.** *There exists a unique weak solution in sense of Definition 2.5 to the Stokes-Darcy phase field formulation problem.*

*Proof.* Because of the regularization (2.4) the proof is similar to the well-posedness proof for the Stokes-Darcy system (e.g. [57, 60]). Therefore, here we just outline the main steps of the proof. We define a function space

$$\mathcal{V}_{div}^\epsilon := \{\mathbf{u} \in \mathcal{V}^\epsilon : \nabla \cdot \mathbf{u} = 0\}.$$

Notice that the solution  $\mathbf{u}$  is an element of  $\mathcal{V}_{div}^\epsilon$ . Now, we define a bilinear form  $a$  on  $\mathcal{V}_{div}^\epsilon \times \mathcal{X}^\epsilon$  as:

$$\begin{aligned} a((\mathbf{u}, p), (\mathbf{v}, \psi)) &:= 2\nu \int_{\Omega} \mathbf{D}(\mathbf{u}) : \mathbf{D}(\mathbf{v})\Phi + \int_{\Omega} \boldsymbol{\kappa} \nabla p \cdot \nabla \psi (1 - \Phi) \\ &+ \int_{\Omega} \psi \mathbf{u} \cdot \nabla \Phi - \int_{\Omega} p \mathbf{v} \cdot \nabla \Phi + \alpha_{BJ} \sum_{i=1}^{d-1} \int_{\Omega} (\mathbf{u} \cdot \tilde{\boldsymbol{\tau}}_i)(\mathbf{v} \cdot \tilde{\boldsymbol{\tau}}_i) |\nabla \Phi|, \end{aligned}$$

and a linear functional  $\mathcal{F}$  as:

$$\langle \mathcal{F}, (\mathbf{v}, \psi) \rangle := \int_{\Omega} \mathbf{F} \cdot \mathbf{v} \Phi + \int_{\Omega} g \psi (1 - \Phi).$$

First we prove the following lemma.

LEMMA 2.7. *The bilinear form  $a(\cdot, \cdot)$  is continuous and coercive on  $\mathcal{V}_{div}^\epsilon \times \mathcal{X}^\epsilon$ .*

*Proof.* In order to show the continuity, special attention has to be given to the terms arising from the coupling at the interface. In particular, using the Cauchy-Schwarz inequality followed by Lemma 2.3, we obtain:

$$\begin{aligned} \int_{\Omega} p \mathbf{v} \cdot \nabla \Phi &\leq \left( \int_{\Omega} |p|^2 |\nabla \Phi| \right)^{\frac{1}{2}} \left( \int_{\Omega} |\mathbf{v}|^2 |\nabla \Phi| \right)^{\frac{1}{2}} \leq \left( \int_{\Omega} |p|^2 |\nabla(1 - \Phi)| \right)^{\frac{1}{2}} \left( \int_{\Omega} |\mathbf{v}|^2 |\nabla \Phi| \right)^{\frac{1}{2}} \\ &\leq C_T \|p\|_{H^1(\Omega, 1-\Phi)} \|\mathbf{v}\|_{H^1(\Omega, \Phi)}. \end{aligned}$$

Similarly, we have

$$\int_{\Omega} \psi \mathbf{u} \cdot \nabla \Phi \leq C_T \|\psi\|_{H^1(\Omega, 1-\Phi)} \|\mathbf{u}\|_{H^1(\Omega, \Phi)},$$

and

$$\begin{aligned} \sum_{i=1}^{d-1} \int_{\Omega} (\mathbf{u} \cdot \tilde{\boldsymbol{\tau}}_i)(\mathbf{v} \cdot \tilde{\boldsymbol{\tau}}_i) |\nabla \Phi| &\leq \sum_{i=1}^{d-1} \left( \int_{\Omega} |\mathbf{u} \cdot \tilde{\boldsymbol{\tau}}_i|^2 |\nabla \Phi| \right)^{\frac{1}{2}} \left( \int_{\Omega} |\mathbf{v} \cdot \tilde{\boldsymbol{\tau}}_i|^2 |\nabla \Phi| \right)^{\frac{1}{2}} \\ &\leq \sum_{i=1}^{d-1} C_T \|\mathbf{u} \cdot \tilde{\boldsymbol{\tau}}_i\|_{H^1(\Omega, \Phi)} \|\mathbf{v} \cdot \tilde{\boldsymbol{\tau}}_i\|_{H^1(\Omega, \Phi)} \leq C_T \|\mathbf{u}\|_{H^1(\Omega, \Phi)} \|\mathbf{v}\|_{H^1(\Omega, \Phi)}. \end{aligned}$$

Other terms can be bounded in the standard way. Therefore, we obtain the following estimate:

$$\begin{aligned} a((\mathbf{u}, p), (\mathbf{v}, \psi)) &\leq 2\nu \|\mathbf{D}(\mathbf{u})\|_{L^2(\Omega, \Phi)} \|\mathbf{D}(\mathbf{v})\|_{L^2(\Omega, \Phi)} + \|\boldsymbol{\kappa} \nabla p\|_{L^2(\Omega, 1-\Phi)} \|\nabla \psi\|_{L^2(\Omega, 1-\Phi)} \\ &+ C_T \|p\|_{H^1(\Omega, 1-\Phi)} \|\mathbf{v}\|_{H^1(\Omega, \Phi)} + C_T \|\psi\|_{H^1(\Omega, 1-\Phi)} \|\mathbf{u}\|_{H^1(\Omega, \Phi)} \\ &+ \alpha_{BJ} C_T \|\mathbf{u}\|_{H^1(\Omega, \Phi)}^2 \|\mathbf{v}\|_{H^1(\Omega, \Phi)}^2 \\ &\leq D \|(\mathbf{u}, p)\|_{\mathcal{V}_{div}^\epsilon \times \mathcal{X}^\epsilon} \|(\mathbf{v}, \psi)\|_{\mathcal{V}_{div}^\epsilon \times \mathcal{X}^\epsilon} \end{aligned}$$

where

$$D = \max\{\alpha_{BJ} C_T, 2\nu, k^*, C_T\}.$$

To show coercivity, we take  $(\mathbf{v}, \psi) = (\mathbf{u}, p)$  to obtain:

$$\begin{aligned} a((\mathbf{u}, p), (\mathbf{u}, p)) &= 2\nu \int_{\Omega} \mathbf{D}(\mathbf{u}) : \mathbf{D}(\mathbf{u})\Phi + \int_{\Omega} \boldsymbol{\kappa} \nabla p \cdot \nabla p (1 - \Phi) + \alpha_{BJ} \sum_{i=1}^{d-1} \int_{\Omega} (\mathbf{u} \cdot \tilde{\boldsymbol{\tau}}_i)^2 |\nabla \Phi| \\ &\geq 2\nu \|\mathbf{D}(\mathbf{u})\|_{L^2(\Omega, \Phi)}^2 + \|\boldsymbol{\kappa}^{\frac{1}{2}} \nabla p\|_{L^2(\Omega, 1-\Phi)}^2. \end{aligned}$$

Using the standard Korn and Poincare inequalities on  $L^2(\Omega)$  together with Lemma 2.2, we have

$$a((\mathbf{u}, p), (\mathbf{u}, p)) \geq D \|(\mathbf{u}, p), (\mathbf{u}, p)\|_{\mathcal{V}_{div}^\epsilon \times \mathcal{X}^\epsilon}^2,$$

where

$$D = \min\left\{\frac{\nu\delta}{C_K^2}, \frac{\nu\delta}{C_P^2 C_K^2}, \frac{k_*}{2}, \frac{k_*\delta}{2C_P^2 C_K^2}\right\},$$

which completes the proof of Lemma 2.7.  $\square$

From estimates analogous to the ones used in Lemma 2.7, it follows that  $\mathcal{F} \in (\mathcal{V}_{div}^\epsilon \times \mathcal{X}^\epsilon)'$ . Therefore, by using standard methods (e.g. Galerkin method), one can easily prove that there exists a unique solution  $(\mathbf{u}, p) \in \mathcal{V}_{div}^\epsilon \times \mathcal{X}^\epsilon$  to the following evolution problem in  $\mathcal{D}'(0, T)$ :

$$(2.6) \quad \frac{d}{dt} \left( \int_{\Omega} \rho \mathbf{u} \cdot \mathbf{v} \Phi + c_0 \int_{\Omega} p \psi (1 - \Phi) \right) + a((\mathbf{u}, p), (\mathbf{v}, \psi)) = \langle \mathcal{F}, (\mathbf{v}, \psi) \rangle, \quad (\mathbf{v}, \psi) \in \mathcal{V}_{div}^\epsilon \times \mathcal{X}^\epsilon.$$

To finish the proof it remains to construct the pressure  $\pi$  corresponding to the solution  $(\mathbf{u}, p)$  of (2.6). This follows in analogous way as in the standard theory of the Navier-Stokes equation. We observe that  $\Phi \nabla \cdot : \mathcal{V}^\epsilon \rightarrow L^2(\Omega)$  is a surjective operator. Namely, because of the regularization (2.4), the equation  $\Phi \nabla \cdot \mathbf{u} = g$  is equivalent to  $\nabla \cdot \mathbf{u} = \frac{g}{\Phi}$ . Therefore, the surjectivity follows directly from the standard Bogovskii theorem (e.g. [61, Section 3.3]). Now, the existence of pressure  $\pi$  can be proved in the same way as in the case of the Navier-Stokes equations (see, e.g., [62, Proposition III.1.1.]).  $\square$

To discretize the problem (2.5) in space, we use the finite element method. Let  $\mathcal{T}_h$  be a conforming triangulation of  $\Omega$  and let  $\mathcal{V}_h^\epsilon \subset \mathcal{V}^\epsilon$ ,  $\mathcal{X}_{F,h}^\epsilon \subset L^2(\Omega)$ ,  $\mathcal{X}_{D,h}^\epsilon \subset \mathcal{X}^\epsilon$ . We assume that the mesh is regular, that the  $h$  is a measure of the grid size, and that the fluid and pressure spaces  $\mathcal{V}_h^\epsilon$  and  $\mathcal{X}_{F,h}^\epsilon$  satisfy the discrete inf-sup condition necessary to ensure the stability of the finite element discretization [63]. We also assume that  $\mathcal{V}_h^\epsilon$  and  $\mathcal{X}_{D,h}^\epsilon$  include piecewise polynomials of degree at least  $k$  and that  $\mathcal{X}_{F,h}^\epsilon$  includes piecewise polynomials of degree  $s \leq k - 1$ .

Let  $t^n = n\Delta t$  for  $n = 0, \dots, N$ , where  $\Delta t$  denotes the time step, and  $T = N\Delta t$  is the final time. For time discretization, we use the backward Euler method. Let  $\psi^n$  denote the approximation of a time-dependent function  $\psi$  at time level  $t^n$ . We will use the following notation for the discrete time derivative:

$$d_t \psi^{n+1} = \frac{\psi^{n+1} - \psi^n}{\Delta t}.$$

The discrete problem is given by: Find  $\mathbf{u}_h^{n+1} \in \mathcal{V}_h^\epsilon$ ,  $\pi_h^{n+1} \in \mathcal{X}_{F,h}^\epsilon$  and  $p_h^{n+1} \in \mathcal{X}_{D,h}^\epsilon$  such that for every  $\mathbf{v}_h \in \mathcal{V}_h^\epsilon$ ,  $\varphi_h \in \mathcal{X}_{F,h}^\epsilon$  and  $\psi_h \in \mathcal{X}_{D,h}^\epsilon$ , we have:

$$(2.7) \quad \begin{aligned} & \rho \int_{\Omega} d_t \mathbf{u}_h^{n+1} \cdot \mathbf{v}_h \Phi + c_0 \int_{\Omega} d_t p_h^{n+1} \psi_h (1 - \Phi) + 2\nu \int_{\Omega} \mathbf{D}(\mathbf{u}_h^{n+1}) : \mathbf{D}(\mathbf{v}_h) \Phi + \int_{\Omega} \kappa \nabla p_h^{n+1} \cdot \nabla \psi_h (1 - \Phi) \\ & - \int_{\Omega} \pi_h^{n+1} \nabla \cdot \mathbf{v}_h \Phi + \int_{\Omega} \varphi_h (\nabla \cdot \mathbf{u}_h^{n+1}) \Phi + \int_{\Omega} \psi_h \mathbf{u}_h^{n+1} \cdot \nabla \Phi - \int_{\Omega} p_h^{n+1} \mathbf{v}_h \cdot \nabla \Phi \\ & + \alpha_{BJ} \sum_{i=1}^{d-1} \int_{\Omega} (\mathbf{u}_h^{n+1} \cdot \tilde{\boldsymbol{\tau}}_i) (\mathbf{v}_h \cdot \tilde{\boldsymbol{\tau}}_i) |\nabla \Phi| = \int_{\Omega} \mathbf{F}_h \cdot \mathbf{v}_h \Phi + \int_{\Omega} g_h \psi_h (1 - \Phi). \end{aligned}$$

**3. Error analysis.** We assume that for the chosen finite element spaces  $\mathcal{V}_h^\epsilon$  and  $\mathcal{X}_{F,h}^\epsilon$ , there exists a projection operator  $P_h : \mathcal{V}^\epsilon \rightarrow \mathcal{V}_h^\epsilon$  satisfying:

$$(3.1) \quad \int_{\Omega} \nabla \cdot (\mathbf{u} - P_h \mathbf{u}) \varphi \Phi = 0 \quad \forall \varphi \in \mathcal{X}_{F,h}^\epsilon, \mathbf{u} \in \mathcal{V}^\epsilon,$$

$$(3.2) \quad \|\mathbf{u} - P_h \mathbf{u}\|_{H^1(\Omega, \Phi)} \leq C \delta^{-\frac{1}{2}} h^k \|\mathbf{u}\|_{H^{k+1}(\Omega, \Phi)} \quad \forall \mathbf{u} \in \mathcal{V}^{k+1},$$

where  $0 \leq s < k$  and  $C$  is a positive constant independent of  $h$  and  $\mathbf{u}$ . Details about the existence of the projection operator in case when  $\Phi = 1$  can be found in [63] for  $k = 1$  and in [64] for  $k = 1, 2, 3$ . Using those results, the relations (3.1)-(3.2) follow from Lemma 2.2. In this section, we assume that  $\delta$  is a fixed, positive number.

Let  $S_h$  be a projection operator onto  $\mathcal{X}_{D,h}^\epsilon$  such that

$$(3.3) \quad \|p - S_h p\|_{H^1(\Omega, 1-\Phi)} \leq C\delta^{-\frac{1}{2}} h^k \|p\|_{H^{k+1}(\Omega, 1-\Phi)} \quad \forall p \in \mathcal{X}_D^{k+1, \epsilon},$$

and let  $R_h$  be a projection operator onto  $\mathcal{X}_{F,h}^\epsilon$  such that

$$(3.4) \quad \|\pi - R_h \pi\|_{L^2(\Omega, \Phi)} \leq C\delta^{-\frac{1}{2}} h^{s+1} \|\pi\|_{H^{s+1}(\Omega, \Phi)} \quad \forall \pi \in \mathcal{X}_F^{k+1, \epsilon},$$

where  $s < k$ .

Let  $a \lesssim (\gtrsim) b$  denote that there exists a positive constant  $C$ , independent  $h$ ,  $\delta$  and  $\Delta t$ , such that  $a \leq (\geq) Cb$ . We introduce the following time discrete norms:

$$\|\mathbf{v}\|_{L^2(0,T;X)} = \left( \Delta t \sum_{n=0}^{N-1} \|\mathbf{v}^{n+1}\|_X^2 \right)^{\frac{1}{2}}, \quad \|\mathbf{v}\|_{L^\infty(0,T;X)} = \max_{0 \leq n \leq N} \|\mathbf{v}^n\|_X,$$

where  $X \in \{H^k(\Omega, \Phi), H^k(\Omega, 1-\Phi)\}$ . Note that they are equivalent to the continuous norms since we use piecewise constant approximations in time. Furthermore, the following inequality holds:

$$\Delta t \sum_{n=1}^{N-1} \|d_t \mathbf{v}^{n+1}\|_X^2 \lesssim \|\partial_t \mathbf{v}\|_{L^2(0,T;X)}^2.$$

The main result of this section is stated in the following theorem.

**THEOREM 3.1.** *Let  $(\mathbf{u}, p, \pi)$  be a solution of (2.5), and let  $\{(\mathbf{u}_h^n, p_h^n, \pi_h^n)\}_{n \geq 1}$  be a solution of (2.7), with discrete initial data*

$$(\mathbf{u}_h^0, p_h^0, \pi_h^0) = (P_h \mathbf{u}^0, S_h p^0, R_h \pi^0).$$

*Then, the following estimate holds:*

$$(3.5) \quad \begin{aligned} & \frac{\rho}{2} \|\mathbf{u}^N - \mathbf{u}_h^N\|_{L^2(\Omega, \Phi)}^2 + \frac{c_0}{2} \|p^N - p_h^N\|_{L^2(\Omega, 1-\Phi)}^2 + \nu \Delta t \sum_{n=0}^{N-1} \|\mathbf{D}(\mathbf{u}^{n+1} - \mathbf{u}_h^{n+1})\|_{L^2(\Omega, \Phi)}^2 \\ & + \frac{k_* \Delta t}{2} \sum_{n=0}^{N-1} \|\nabla(p^{n+1} - p_h^{n+1})\|_{L^2(\Omega, 1-\Phi)}^2 \\ & \lesssim \Delta t^2 \left( \frac{\rho_P^2 C_P^2 C_K^2}{\nu \delta} \|\partial_{tt} \mathbf{u}\|_{L^2(0,T;L^2(\Omega, \Phi))}^2 + \frac{c_0^2 C_P^2}{k_*} \|\partial_{tt} p\|_{L^2(0,T;L^2(\Omega, 1-\Phi))}^2 \right) \\ & + h^{2k} \left( \frac{\rho}{\delta} \|\mathbf{u}\|_{L^\infty(0,T;H^{k+1}(\Omega, \Phi))}^2 + \frac{\rho^2 C_P^2 C_K^2}{\nu \delta^2} \|\partial_t \mathbf{u}\|_{L^2(0,T;H^{k+1}(\Omega, \Phi))}^2 \right) \\ & + \left( \frac{\nu}{\delta} + \frac{C_T^4 (C_P^2 + 1)}{k_* \delta} + \frac{\alpha_{BJ}^2 C_T^4 C_K^2}{\delta^2} (C_P^2 + 1) \right) \|\mathbf{u}\|_{L^2(0,T;H^{k+1}(\Omega, \Phi))}^2 + \frac{c_0}{\delta} \|p\|_{L^\infty(0,T;H^{k+1}(\Omega, 1-\Phi))}^2 \\ & + \left( \frac{c_0^2 C_P^2}{k_* \delta} + \frac{(k^*)^2}{k_* \delta} + \frac{C_T^4 C_K^2}{\nu \delta^2} (C_P^2 + 1) \right) \|p\|_{L^2(0,T;H^{k+1}(\Omega, 1-\Phi))}^2 \\ & + h^{2s+2} \frac{d C_K^2}{\nu \delta^2} \|\pi\|_{L^2(0,T;H^{s+1}(\Omega, \Phi))}^2. \end{aligned}$$

*Proof.* Define  $\mathbf{e}_U = \mathbf{u} - \mathbf{u}_h$ ,  $e_\pi = \pi - \pi_h$  and  $e_P = p - p_h$ . We begin by subtracting (2.7) from (2.5), obtaining the following error equation:

$$\begin{aligned} & \rho \int_{\Omega} d_t \mathbf{e}_U^{n+1} \cdot \mathbf{v}_h \Phi + 2\nu \int_{\Omega} \mathbf{D}(\mathbf{e}_U^{n+1}) : \mathbf{D}(\mathbf{v}_h) \Phi - \int_{\Omega} e_\pi^{n+1} \nabla \cdot \mathbf{v}_h \Phi + \int_{\Omega} \varphi_h \nabla \cdot \mathbf{e}_U^{n+1} \Phi \\ & + c_0 \int_{\Omega} d_t e_P^{n+1} \psi_h (1-\Phi) + \int_{\Omega} \kappa \nabla e_P^{n+1} \cdot \nabla \psi_h (1-\Phi) - \int_{\Omega} e_P^{n+1} \mathbf{v}_h \cdot \nabla \Phi \end{aligned}$$



$$(3.6) \quad + \int_{\Omega} \psi_h \mathbf{e}_U^{n+1} \cdot \nabla \Phi + \alpha_{BJ} \sum_{i=1}^{d-1} \int_{\Omega} (\mathbf{e}_U^{n+1} \cdot \tilde{\boldsymbol{\tau}}_i)(\mathbf{v}_h \cdot \tilde{\boldsymbol{\tau}}_i) |\nabla \Phi| = \mathcal{R}(\mathbf{v}_h \psi_h),$$

where

$$\mathcal{R}(\mathbf{v}_h, \psi_h) = \rho_F \int_{\Omega} (d_t \mathbf{u}^{n+1} - \partial_t \mathbf{u}^{n+1}) \cdot \mathbf{v}_h \Phi + c_0 \int_{\Omega} (d_t p^{n+1} - \partial_t p^{n+1}) \psi_h (1 - \Phi).$$

We decompose the error into the sum of the interpolation error and the approximation error as:

$$\begin{aligned} \mathbf{e}_U &= \mathbf{u} - P_h \mathbf{u} + P_h \mathbf{u} - \mathbf{u}_h = \boldsymbol{\theta}_U + \boldsymbol{\delta}_U, \\ e_{\pi} &= \pi - R_h \pi + R_h \pi - \pi_h = \theta_{\pi} + \delta_{\pi}, \\ e_P &= p - S_h p + S_h p - p_h = \theta_P + \delta_P. \end{aligned}$$

Let  $\mathbf{v}_h = \boldsymbol{\delta}_U^{n+1}$ ,  $\varphi_h = \delta_{\pi}^{n+1}$ ,  $\psi_h = \delta_P^{n+1}$  in (3.6). Then, we obtain:

$$\begin{aligned} & \frac{\rho}{2\Delta t} \left( \|\boldsymbol{\delta}_U^{n+1}\|_{L^2(\Omega, \Phi)}^2 - \|\boldsymbol{\delta}_U^n\|_{L^2(\Omega, \Phi)}^2 + \|\boldsymbol{\delta}_U^{n+1} - \boldsymbol{\delta}_U^n\|_{L^2(\Omega, \Phi)}^2 \right) + 2\nu \|\mathbf{D}(\boldsymbol{\delta}_U^{n+1})\|_{L^2(\Omega, \Phi)}^2 \\ & + \frac{c_0}{2\Delta t} \left( \|\delta_P^{n+1}\|_{L^2(\Omega, 1-\Phi)}^2 - \|\delta_P^n\|_{L^2(\Omega, 1-\Phi)}^2 + \|\delta_P^{n+1} - \delta_P^n\|_{L^2(\Omega, 1-\Phi)}^2 \right) + \|\boldsymbol{\kappa}^{\frac{1}{2}} \nabla \delta_P^{n+1}\|_{L^2(\Omega, 1-\Phi)}^2 \\ & \quad + \alpha_{BJ} \sum_{i=1}^{d-1} \int_{\Omega} |\boldsymbol{\delta}_U^{n+1} \cdot \tilde{\boldsymbol{\tau}}_i|^2 |\nabla \Phi| \\ & = \mathcal{R}(\boldsymbol{\delta}_U^{n+1}, \delta_P^{n+1}) - \int_{\Omega} \rho d_t \boldsymbol{\theta}_U^{n+1} \cdot \boldsymbol{\delta}_U^{n+1} \Phi - \int_{\Omega} 2\nu \mathbf{D}(\boldsymbol{\theta}_U^{n+1}) : \mathbf{D}(\boldsymbol{\delta}_U^{n+1}) \Phi + \int_{\Omega} \theta_{\pi}^{n+1} (\nabla \cdot \boldsymbol{\delta}_U^{n+1}) \Phi \\ & \quad - \int_{\Omega} \delta_{\pi}^{n+1} (\nabla \cdot \boldsymbol{\theta}_U^{n+1}) \Phi - \int_{\Omega} c_0 d_t \theta_P^{n+1} \delta_P^{n+1} (1 - \Phi) - \int_{\Omega} \boldsymbol{\kappa} \nabla \theta_P^{n+1} \cdot \nabla \delta_P^{n+1} (1 - \Phi) \\ (3.7) \quad & - \int_{\Omega} \theta_P^{n+1} \delta_U^{n+1} \cdot \nabla \Phi + \int_{\Omega} \delta_P^{n+1} \boldsymbol{\theta}_U^{n+1} \cdot \nabla \Phi - \alpha_{BJ} \sum_{i=1}^{d-1} \int_{\Omega} (\boldsymbol{\theta}_U^{n+1} \cdot \tilde{\boldsymbol{\tau}}_i) (\delta_U^{n+1} \cdot \tilde{\boldsymbol{\tau}}_i) |\nabla \Phi|. \end{aligned}$$

Thanks to (3.1), we have

$$\int_{\Omega} \delta_{\pi}^{n+1} (\nabla \cdot \boldsymbol{\theta}_U^{n+1}) \Phi = 0.$$

We bound the right-hand side as follows. Using the Cauchy-Schwarz and Young's inequalities, we obtain:

$$\begin{aligned} & \int_{\Omega} \rho d_t \boldsymbol{\theta}_U^{n+1} \cdot \boldsymbol{\delta}_U^{n+1} \Phi + \int_{\Omega} 2\nu \mathbf{D}(\boldsymbol{\theta}_U^{n+1}) : \mathbf{D}(\boldsymbol{\delta}_U^{n+1}) \Phi + \int_{\Omega} \theta_{\pi}^{n+1} (\nabla \cdot \boldsymbol{\delta}_U^{n+1}) \Phi + \int_{\Omega} c_0 d_t \theta_P^{n+1} \delta_P^{n+1} (1 - \Phi) \\ & \quad + \int_{\Omega} \boldsymbol{\kappa} \nabla \theta_P^{n+1} \cdot \nabla \delta_P^{n+1} (1 - \Phi) \\ & \lesssim \frac{\nu \delta}{C_P^2 C_K^2} \|\boldsymbol{\delta}_U^{n+1}\|_{L^2(\Omega, \Phi)}^2 + \frac{\rho^2 C_P^2 C_K^2}{\nu \delta} \|d_t \boldsymbol{\theta}_U^{n+1}\|_{L^2(\Omega, \Phi)}^2 + \nu \|\mathbf{D}(\boldsymbol{\delta}_U^{n+1})\|_{L^2(\Omega, \Phi)}^2 + \nu \|\mathbf{D}(\boldsymbol{\theta}_U^{n+1})\|_{L^2(\Omega, \Phi)}^2 \\ & \quad + \frac{d C_K^2}{\nu \delta} \|\theta_{\pi}^{n+1}\|_{L^2(\Omega, \Phi)}^2 + \frac{\nu \delta}{d C_K^2} \|\nabla \cdot \boldsymbol{\delta}_U^{n+1}\|_{L^2(\Omega, \Phi)}^2 + \frac{k_*}{C_P^2} \|\delta_P^{n+1}\|_{L^2(\Omega, 1-\Phi)}^2 + \frac{c_0^2 C_P^2}{2k_*} \|\theta_P^{n+1}\|_{L^2(\Omega, 1-\Phi)}^2 \\ & \quad + k_* \|\nabla \delta_P^{n+1}\|_{L^2(\Omega, 1-\Phi)}^2 + \frac{(k^*)^2}{k_*} \|\nabla \theta_P^{n+1}\|_{L^2(\Omega, 1-\Phi)}^2. \end{aligned}$$

Using Lemma 2.3, Young's inequality with  $\epsilon = \frac{C_T^2 C_K^2}{\nu \delta} (C_P^2 + 1)$ , Lemma 2.4 and Korn's inequality combined with Lemma 2.2, we can estimate:

$$\left| \int_{\Omega} \theta_P^{n+1} \boldsymbol{\delta}_U^{n+1} \cdot \nabla \Phi \right| \leq \left( \int_{\Omega} |\theta_P^{n+1}|^2 |\nabla \Phi| \right)^{\frac{1}{2}} \left( \int_{\Omega} |\boldsymbol{\delta}_U^{n+1}|^2 |\nabla \Phi| \right)^{\frac{1}{2}}$$

$$\begin{aligned}
&\leq \left( \int_{\Omega} |\theta_P^{n+1}|^2 |\nabla(1-\Phi)| \right)^{\frac{1}{2}} \left( \int_{\Omega} |\delta_U^{n+1}|^2 |\nabla\Phi| \right)^{\frac{1}{2}} \\
&\leq C_T^2 \|\theta_P^{n+1}\|_{H^1(\Omega, 1-\Phi)} \|\delta_U^{n+1}\|_{H^1(\Omega, \Phi)} \\
&\leq \frac{C_T^2 \epsilon}{2} \|\theta_P^{n+1}\|_{H^1(\Omega, 1-\Phi)}^2 + \frac{C_T^2}{2\epsilon} \|\delta_U^{n+1}\|_{H^1(\Omega, \Phi)}^2 \\
&\lesssim \frac{C_T^4 C_K^2}{\nu \delta} (C_P^2 + 1) \|\theta_P^{n+1}\|_{H^1(\Omega, 1-\Phi)}^2 + \nu \|\mathbf{D}(\delta_U^{n+1})\|_{L^2(\Omega, \Phi)}^2,
\end{aligned}$$

and, similarly,

$$\int_{\Omega} \delta_P^{n+1} \theta_U^{n+1} \cdot \nabla\Phi \lesssim k_* \|\nabla \delta_P^{n+1}\|_{L^2(\Omega, 1-\Phi)}^2 + \frac{C_T^4 (C_P^2 + 1)}{k_*} \|\theta_U^{n+1}\|_{H^1(\Omega, \Phi)}^2,$$

and

$$\alpha_{BJ} \sum_{i=1}^{d-1} \int_{\Omega} (\theta_U^{n+1} \cdot \tilde{\tau}_i) (\delta_U^{n+1} \cdot \tilde{\tau}_i) |\nabla\Phi| \lesssim \frac{\alpha_{BJ}^2 C_T^4 C_K^2}{\delta} (C_P^2 + 1) \|\theta_U^{n+1}\|_{H^1(\Omega, \Phi)}^2 + \nu \|\mathbf{D}(\delta_U^{n+1})\|_{L^2(\Omega, \Phi)}^2.$$

Using Lemma 2.4, Korn's inequality combined with Lemma 2.2, and

$$\|\nabla \cdot \delta_U^{n+1}\|_{L^2(\Omega, \Phi)}^2 \leq \frac{d C_K^2}{\delta} \|\mathbf{D}(\delta_U^{n+1})\|_{L^2(\Omega, \Phi)}^2,$$

and combining the results above with (3.7), we get:

$$\begin{aligned}
&\frac{\rho}{2\Delta t} \left( \|\delta_U^{n+1}\|_{L^2(\Omega, \Phi)}^2 - \|\delta_U^n\|_{L^2(\Omega, \Phi)}^2 + \|\delta_U^{n+1} - \delta_U^n\|_{L^2(\Omega, \Phi)}^2 \right) + \nu \|\mathbf{D}(\delta_U^{n+1})\|_{L^2(\Omega, \Phi)}^2 \\
&\quad + \frac{c_0}{2\Delta t} \left( \|\delta_P^{n+1}\|_{L^2(\Omega, 1-\Phi)}^2 - \|\delta_P^n\|_{L^2(\Omega, 1-\Phi)}^2 + \|\delta_P^{n+1} - \delta_P^n\|_{L^2(\Omega, 1-\Phi)}^2 \right) \\
&\quad + \frac{k_*}{2} \|\nabla \delta_P^{n+1}\|_{L^2(\Omega, 1-\Phi)}^2 + \alpha_{BJ} \sum_{i=1}^{d-1} \int_{\Omega} |\delta_U^{n+1} \cdot \tilde{\tau}_i|^2 |\nabla\Phi| \\
&\lesssim \mathcal{R}(\delta_U^{n+1}, \delta_P^{n+1}) + \frac{\rho^2 C_P^2 C_K^2}{\nu \delta} \|d_t \theta_U^{n+1}\|_{L^2(\Omega, \Phi)}^2 + \nu \|\mathbf{D}(\theta_U^{n+1})\|_{L^2(\Omega, \Phi)}^2 + \frac{d C_K^2}{\nu \delta} \|\theta_U^{n+1}\|_{L^2(\Omega, \Phi)}^2 \\
&\quad + \frac{c_0^2 C_P^2}{k_*} \|\theta_P^{n+1}\|_{L^2(\Omega, 1-\Phi)}^2 + \frac{(k^*)^2}{k_*} \|\nabla \theta_P^{n+1}\|_{L^2(\Omega, 1-\Phi)}^2 + \frac{C_T^4 C_K^2}{\nu \delta} (C_P^2 + 1) \|\theta_P^{n+1}\|_{H^1(\Omega, 1-\Phi)}^2 \\
&\quad + \frac{C_T^4 (C_P^2 + 1)}{k_*} \|\theta_U^{n+1}\|_{H^1(\Omega, \Phi)}^2 + \frac{\alpha_{BJ}^2 C_T^4 C_K^2}{\delta} (C_P^2 + 1) \|\theta_U^{n+1}\|_{H^1(\Omega, \Phi)}^2.
\end{aligned}$$

Discarding a positive term on the left-hand side, summing from  $n = 0$  to  $N - 1$ , multiplying by  $\Delta t$  and using the approximation properties (3.2)-(3.4), we obtain:

$$\begin{aligned}
&\frac{\rho}{2} \|\delta_U^N\|_{L^2(\Omega, \Phi)}^2 + \frac{c_0}{2} \|\delta_P^N\|_{L^2(\Omega, 1-\Phi)}^2 + \nu \Delta t \sum_{n=0}^{N-1} \|\mathbf{D}(\delta_U^{n+1})\|_{L^2(\Omega, \Phi)}^2 + \frac{\rho \Delta t^2}{2} \sum_{n=0}^{N-1} \|d_t \delta_U^{n+1}\|_{L^2(\Omega, \Phi)}^2 \\
&\quad + \frac{c_0 \Delta t^2}{2} \sum_{n=0}^{N-1} \|d_t \delta_P^{n+1}\|_{L^2(\Omega, 1-\Phi)}^2 + \frac{k_* \Delta t}{2} \sum_{n=0}^{N-1} \|\nabla \delta_P^{n+1}\|_{L^2(\Omega, 1-\Phi)}^2 \\
&\lesssim \Delta t \sum_{n=0}^{N-1} \mathcal{R}(\delta_U^{n+1}, \delta_P^{n+1}) + \frac{\rho^2 C_P^2 C_K^2}{\nu \delta^2} h^{2k} \|\partial_t \mathbf{u}\|_{L^2(0, T; H^{k+1}(\Omega, \Phi))}^2 + \frac{\nu}{\delta} h^{2k} \|\mathbf{u}\|_{L^2(0, T; H^{k+1}(\Omega, \Phi))}^2 \\
&\quad + \frac{C_T^4 (C_P^2 + 1)}{k_* \delta} h^{2k} \|\mathbf{u}\|_{L^2(0, T; H^{k+1}(\Omega, \Phi))}^2 + \frac{\alpha_{BJ}^2 C_T^4 C_K^2}{\delta^2} (C_P^2 + 1) h^{2k} \|\mathbf{u}\|_{L^2(0, T; H^{k+1}(\Omega, \Phi))}^2 \\
&\quad + \frac{d C_K^2}{\nu \delta^2} h^{2s+2} \|\pi\|_{L^2(0, T; H^{s+1}(\Omega, \Phi))}^2 + \frac{c_0^2 C_P^2}{k_* \delta} h^{2k} \|p\|_{L^2(0, T; H^{k+1}(\Omega, 1-\Phi))}^2
\end{aligned}$$

$$+ \frac{(k^*)^2}{k_* \delta} h^{2k} \|p\|_{L^2(0,T;H^{k+1}(\Omega,1-\Phi))}^2 + \frac{C_T^4 C_K^2}{\nu \delta^2} (C_P^2 + 1) h^{2k} \|p\|_{L^2(0,T;H^{k+1}(\Omega,1-\Phi))}^2.$$

Finally, using Lemma 3.2 to estimate the residual term  $\mathcal{R}(\delta_U^{n+1}, \delta_P^{n+1})$ , we have:

$$\begin{aligned} & \frac{\rho}{2} \|\delta_U^N\|_{L^2(\Omega,\Phi)}^2 + \frac{c_0}{2} \|\delta_P^N\|_{L^2(\Omega,1-\Phi)}^2 + \nu \Delta t \sum_{n=0}^{N-1} \|\mathbf{D}(\delta_U^{n+1})\|_{L^2(\Omega,\Phi)}^2 + \frac{\rho \Delta t^2}{2} \sum_{n=0}^{N-1} \|d_t \delta_U^{n+1}\|_{L^2(\Omega,\Phi)}^2 \\ & \quad + \frac{c_0 \Delta t^2}{2} \sum_{n=0}^{N-1} \|d_t \delta_P^{n+1}\|_{L^2(\Omega,1-\Phi)}^2 + \frac{k_* \Delta t}{2} \sum_{n=0}^{N-1} \|\nabla \delta_P^{n+1}\|_{L^2(\Omega,1-\Phi)}^2 \\ & \lesssim \Delta t^2 \left( \frac{\rho_F^2 C_P^2 C_K^2}{\nu \delta} \|\partial_{tt} \mathbf{u}\|_{L^2(0,T;L^2(\Omega,\Phi))}^2 + \frac{c_0^2 C_P^2}{k_*} \|\partial_{tt} p\|_{L^2(0,T;L^2(\Omega,1-\Phi))}^2 \right) \\ & \quad + h^{2k} \frac{\rho^2 C_P^2 C_K^2}{\nu \delta^2} \|\partial_t \mathbf{u}\|_{L^2(0,T;H^{k+1}(\Omega,\Phi))}^2 \\ & \quad + h^{2k} \left( \frac{\nu}{\delta} + \frac{C_T^4 (C_P^2 + 1)}{k_* \delta} + \frac{\alpha_{BJ}^2 C_T^4 C_K^2}{\delta^2} (C_P^2 + 1) \right) \|\mathbf{u}\|_{L^2(0,T;H^{k+1}(\Omega,\Phi))}^2 \\ & \quad + h^{2k} \left( \frac{c_0^2 C_P^2}{k_* \delta} + \frac{(k^*)^2}{k_* \delta} + \frac{C_T^4 C_K^2}{\nu \delta^2} (C_P^2 + 1) \right) \|p\|_{L^2(0,T;H^{k+1}(\Omega,1-\Phi))}^2 \\ & \quad + h^{2s+2} \frac{dC_K^2}{\nu \delta^2} \|\pi\|_{L^2(0,T;H^{s+1}(\Omega,\Phi))}^2. \quad \square \end{aligned}$$

The final estimate follows from the triangle inequality.

In the following, we state and prove two lemmas that were used in the proof of Theorem 3.1.

LEMMA 3.2. *The following estimate holds:*

$$\begin{aligned} & \Delta t \sum_{n=0}^{N-1} \mathcal{R}(\delta_U^{n+1}, \delta_P^{n+1}) \\ & \lesssim \Delta t^2 \left( \frac{\rho_F^2 C_P^2 C_K^2}{\nu \delta} \|\partial_{tt} \mathbf{u}\|_{L^2(0,T;L^2(\Omega,\Phi))}^2 + \frac{c_0^2 C_P^2}{k_*} \|\partial_{tt} p\|_{L^2(0,T;L^2(\Omega,1-\Phi))}^2 \right) \\ & \quad + \nu \Delta t \sum_{n=0}^{N-1} \|\mathbf{D}(\delta_U^{n+1})\|_{L^2(\Omega,\Phi)}^2 + k_* \Delta t \sum_{n=0}^{N-1} \|\nabla \delta_P^{n+1}\|_{L^2(\Omega,1-\Phi)}^2. \end{aligned}$$

*Proof.* Using the Cauchy-Schwartz, Young's, the Poincaré - Friedrichs, and Korn's inequalities, we have:

$$\begin{aligned} & \Delta t \sum_{n=0}^{N-1} \mathcal{R}(\delta_U^{n+1}, \delta_P^{n+1}) = \\ & \Delta t \rho_F \sum_{n=0}^{N-1} \int_{\Omega} (d_t \mathbf{u}^{n+1} - \partial_t \mathbf{u}^{n+1}) \cdot \delta_U^{n+1} \Phi + \Delta t c_0 \sum_{n=0}^{N-1} \int_{\Omega} (d_t p^{n+1} - \partial_t p^{n+1}) \delta_P^{n+1} (1 - \Phi) \\ & \lesssim \frac{\Delta t \rho_F^2 C_P^2 C_K^2}{\nu \delta} \sum_{n=0}^{N-1} \|d_t \mathbf{u}^{n+1} - \partial_t \mathbf{u}^{n+1}\|_{L^2(\Omega,\Phi)}^2 + \nu \Delta t \sum_{n=0}^{N-1} \|\mathbf{D}(\delta_U^{n+1})\|_{L^2(\Omega,\Phi)}^2 \\ & \quad + \frac{\Delta t c_0^2 C_P^2}{k_*} \sum_{n=0}^{N-1} \|d_t p^{n+1} - \partial_t p^{n+1}\|_{L^2(\Omega,1-\Phi)}^2 + \Delta t k_* \sum_{n=0}^{N-1} \|\nabla \delta_P^{n+1}\|_{L^2(\Omega,1-\Phi)}^2. \end{aligned}$$

The final estimate follows by applying Lemma 3.3. □

LEMMA 3.3 (Consistency errors). *Let  $\omega$  be a weight. Then, the following inequality holds:*

$$\Delta t \sum_{n=0}^{N-1} \|d_t \mathbf{v}^{n+1} - \partial_t \mathbf{v}^{n+1}\|_{L^2(\Omega,\omega)}^2 \lesssim \Delta t^2 \|\partial_{tt} \mathbf{v}\|_{L^2(0,T;L^2(\Omega,\omega))}^2.$$

*Proof.* Using the Cauchy-Schwartz inequality, we have:

$$\begin{aligned}
& \Delta t \sum_{n=0}^{N-1} \|d_t \mathbf{v}^{n+1} - \partial_t \mathbf{v}^{n+1}\|_{L^2(\Omega, \omega)}^2 \\
&= \Delta t \sum_{n=0}^{N-1} \int_{\Omega} \left| \frac{1}{\Delta t} \int_{t^n}^{t^{n+1}} (t - t^n) \partial_{tt} \mathbf{v}(t) dt \right|^2 \omega dx \\
&\leq \frac{1}{\Delta t} \int_{\Omega} \sum_{n=0}^{N-1} \left( \int_{t^n}^{t^{n+1}} |t - t^n|^2 dt \int_{t^n}^{t^{n+1}} |\partial_{tt} \mathbf{v}|^2 dt \right) \omega dx \\
&\leq \frac{\Delta t^2}{3} \int_{\Omega} \int_0^T |\partial_{tt} \mathbf{v}|^2 dt \omega dx \lesssim \Delta t^2 \|\partial_{tt} \mathbf{v}\|_{L^2(0, T; L^2(\Omega, \omega))}^2. \quad \square
\end{aligned}$$

**REMARK 3.1.** *In the proofs of Theorems 2.6 and 3.1, we heavily used the fact that the phase field function is strictly greater than  $\delta$  due to the regularization (2.4). The parameter  $\delta$  was assumed to be fixed, i.e. independent of the discretization parameters, and small. In the proof of Theorem 2.6, it was essential that  $\delta > 0$ . Even though the constants in the error estimates proved in Theorem 3.1 depend on the negative powers of  $\delta$ , the estimates are still valuable because  $h$  and  $\Delta t$  can be chosen as powers of  $\delta$  so that the right-hand side is guaranteed to converge to 0 as  $\delta \rightarrow 0$ . Moreover, the numerical experiments suggest that the actual numerical error is independent of the regularization parameter,  $\delta$ , see Section 5. However, the proof of the well-posedness for  $\delta = 0$  is much more involved and relies on the theory of weighted spaces with Muckenhoupt weights (see e.g. [65–67]). This is outside of the scope of this paper and will be addressed in our forthcoming work.*

**4. Modeling error.** In this section, we estimate the difference between the continuous solutions of the diffuse and sharp interface formulations in terms of the parameter  $\epsilon$  describing the diffuse interface width (see definition of the phase field function in Section 2.2). For simplicity, in this section we assume that there is no regularization, i.e.  $\delta = 0$ . Moreover, to make the exposition more clear, we slightly change the notation and introduce subscripts “s” and “d” to denote the solutions to the sharp interface and the diffuse interface formulations, respectively.

The weak solution,  $(\mathbf{u}_s, p_s)$ , to the sharp interface problem satisfies the following weak form (see Definition 2.1):

$$\begin{aligned}
(4.1) \quad & \rho \int_{\Omega_F} \partial_t \mathbf{u}_s \cdot \mathbf{v} + c_0 \int_{\Omega_D} \partial_t p_s \psi + \int_{\Omega_F} \boldsymbol{\sigma}(\nabla \mathbf{u}_s, \pi_s) : \nabla \mathbf{v} + \int_{\Omega_D} \boldsymbol{\kappa} \nabla p_s \cdot \nabla \psi \\
& + \int_{\Gamma} p_s \mathbf{v} \cdot \mathbf{n} - \int_{\Gamma} \psi \mathbf{u}_s \cdot \mathbf{n} + \alpha_{BJ} \sum_{i=0}^{d-1} \int_{\Gamma} (\mathbf{u}_s \cdot \boldsymbol{\tau}_i)(\mathbf{v} \cdot \boldsymbol{\tau}_i) = \int_{\Omega_F} \mathbf{F} \cdot \mathbf{v} + \int_{\Omega_D} g \psi, \quad (\mathbf{v}, \psi) \in \mathcal{V}_{div} \times \mathcal{X}.
\end{aligned}$$

Here subscript *div* in  $\mathcal{V}_{div}$  denotes the space of divergence free functions. The continuous diffuse interface solution, with the diffuse layer of width  $\approx \epsilon$ , is denoted by  $(\mathbf{u}_d^\epsilon, p_d^\epsilon)$ , and satisfies the following weak form (Definition 2.5):

$$\begin{aligned}
(4.2) \quad & \rho \int_{\Omega} \partial_t \mathbf{u}_d^\epsilon \cdot \mathbf{v} \Phi^\epsilon + c_0 \int_{\Omega} (\partial_t p_d^\epsilon \psi)(1 - \Phi^\epsilon) + \int_{\Omega} (\boldsymbol{\sigma}(\nabla \mathbf{u}_d^\epsilon, \pi_d^\epsilon) : \nabla \mathbf{v}) \Phi^\epsilon + \int_{\Omega} \boldsymbol{\kappa} \nabla p_d^\epsilon \cdot \nabla \psi (1 - \Phi^\epsilon) \\
& - \int_{\Omega} p_d^\epsilon \mathbf{v} \cdot \nabla \Phi^\epsilon + \int_{\Omega} \psi \mathbf{u}_d^\epsilon \cdot \nabla \Phi^\epsilon + \alpha_{BJ} \sum_{i=0}^{d-1} \int_{\Omega} (\mathbf{u}_d^\epsilon \cdot \tilde{\boldsymbol{\tau}}_i)(\mathbf{v} \cdot \tilde{\boldsymbol{\tau}}_i) |\nabla \Phi^\epsilon| = \int_{\Omega} \mathbf{F} \cdot \mathbf{v} \Phi^\epsilon + \int_{\Omega} g \psi (1 - \Phi^\epsilon),
\end{aligned}$$

for all test function  $(\mathbf{v}, \psi) \in \mathcal{V}_{div} \times \mathcal{X}^\epsilon$ . Our goal is to estimate  $\|(\mathbf{u}_s, p_s) - (\mathbf{u}_d^\epsilon, p_d^\epsilon)\|$  in a suitable norm, in terms of powers of  $\epsilon$ . This will be done by subtracting the weak form of the diffuse interface formulation from the weak form of the sharp interface formulation, taking suitable test functions, and using the convergence properties of the diffuse integrals.

THEOREM 4.1. Let  $(\mathbf{u}_s, p_s, \pi_s)$  be a solution of the sharp interface Stokes-Darcy problem in the sense of Definition 2.1, and  $(\mathbf{u}_d^\epsilon, p_d^\epsilon, \pi_d^\epsilon)$  be a solution of the diffuse interface problem in sense of Definition 2.5. Furthermore, assume  $\mathbf{F} \in H^1(\Omega)$ ,  $g \in H^1(\Omega)$  and

$$\begin{aligned} (\mathbf{u}_s, \pi_s) &\in (H^1(0, T; W^{1,\infty}(\Omega)) \times L^2(0, T; W^{3,\infty}(\Omega))) \times L^2(0, T; W^{2,\infty}(\Omega)), \\ p_s &\in H^1(0, T; W^{1,\infty}(\Omega)) \times L^2(0, T; W^{3,\infty}(\Omega)). \end{aligned}$$

Then, there exists a constant  $C$  independent of  $\epsilon$  such that the following estimate holds:

$$\begin{aligned} (4.3) \quad &\rho \|\mathbf{u}_s - \mathbf{u}_d^\epsilon\|_{L^\infty(0, T; L^2(\Omega, \Phi^\epsilon))}^2 + c_0 \|p_s - p_d^\epsilon\|_{L^\infty(0, T; L^2(1 - \Phi^\epsilon))}^2 + \nu \|\mathbf{D}(\mathbf{u}_s - \mathbf{u}_d^\epsilon)\|_{L^2(0, T; L^2(\Omega, \Phi^\epsilon))} \\ &+ \frac{\kappa}{2} \|\nabla(p_s - p_d^\epsilon)\|_{L^2(0, T; L^2(\Omega, 1 - \Phi^\epsilon))} + \alpha_{BJ} \sum_{i=0}^{d-1} \int_0^T \int_\Omega |(\mathbf{u}_s - \mathbf{u}_d^\epsilon) \cdot \tilde{\tau}_i|^2 |\nabla \Phi^\epsilon| \\ &\lesssim \epsilon^3 \left( \|\partial_t \mathbf{u}_s\|_{L^2(0, T; W^{1,\infty}(\Omega))}^2 + \|\partial_t p_s\|_{L^2(0, T; W^{1,\infty}(\Omega))}^2 \right) \\ &+ \|\mathbf{u}_s\|_{L^2(0, T; W^{3,\infty}(\Omega))}^2 + \|\pi_s\|_{L^2(0, T; W^{2,\infty}(\Omega))}^2 + \|p_s\|_{L^2(0, T; W^{3,\infty}(\Omega))}^2 \end{aligned}$$

*Proof.* We begin by subtracting (4.2) from (4.1). Using a divergence-free extension operator to extended the sharp interface solution to the whole domain, we obtaining the following equation:

$$\begin{aligned} &\rho \int_\Omega \partial_t (\mathbf{u}_s - \mathbf{u}_d^\epsilon) \cdot \mathbf{v} \Phi^\epsilon + \rho \int_\Omega \partial_t \mathbf{u}_s \cdot \mathbf{v} (\chi - \Phi^\epsilon) + c_0 \int_\Omega \partial_t (p_s - p_d^\epsilon) \psi (1 - \Phi^\epsilon) + c_0 \int_\Omega \partial_t p_s \psi (\Phi^\epsilon - \chi) \\ &+ \int_\Omega \boldsymbol{\sigma} (\nabla (\mathbf{u}_s - \mathbf{u}_d^\epsilon), \pi_s - \pi_d^\epsilon) : \nabla \mathbf{v} \Phi^\epsilon + \int_\Omega \boldsymbol{\sigma} (\nabla \mathbf{u}_s, \pi_s) : \nabla \mathbf{v} (\chi - \Phi^\epsilon) + \kappa \int_\Omega \nabla (p_s - p_d^\epsilon) \cdot \nabla \psi (1 - \Phi^\epsilon) \\ &+ \kappa \int_\Omega \nabla p_s \cdot \nabla \psi (\Phi^\epsilon - \chi) + \int_\Gamma p_s \mathbf{v} \cdot \mathbf{n} - \int_\Gamma \psi \mathbf{u}_s \cdot \mathbf{n} + \alpha_{BJ} \sum_{i=0}^{d-1} \int_\Gamma (\mathbf{u}_s \cdot \boldsymbol{\tau}_i) (\mathbf{v} \cdot \boldsymbol{\tau}_i) \\ &+ \int_\Omega p_d^\epsilon \mathbf{v} \cdot \nabla \Phi^\epsilon - \int_\Omega \psi \mathbf{u}_d^\epsilon \cdot \nabla \Phi^\epsilon - \alpha_{BJ} \sum_{i=0}^{d-1} \int_\Omega (\mathbf{u}_d^\epsilon \cdot \tilde{\tau}_i) (\mathbf{v} \cdot \tilde{\tau}_i) |\nabla \Phi^\epsilon| = \int_\Omega (\mathbf{F} \cdot \mathbf{v} - g \psi) (\chi - \Phi^\epsilon). \end{aligned}$$

Taking  $(\mathbf{v}, \psi) = (\mathbf{u}_s - \mathbf{u}_d^\epsilon, p_s - p_d^\epsilon) =: (\mathbf{v}^\epsilon, \psi^\epsilon)$ , we get:

$$\begin{aligned} (4.4) \quad &\frac{1}{2} \frac{d}{dt} \left( \rho \|\mathbf{u}_s - \mathbf{u}_d^\epsilon\|_{L^2(\Omega, \Phi^\epsilon)}^2 + c_0 \|p_s - p_d^\epsilon\|_{L^2(\Omega, 1 - \Phi^\epsilon)}^2 \right) + 2\nu \|\mathbf{D}(\mathbf{u}_s - \mathbf{u}_d^\epsilon)\|_{L^2(\Omega, \Phi^\epsilon)}^2 + \kappa \|\nabla(p_s - p_d^\epsilon)\|_{L^2(\Omega, 1 - \Phi^\epsilon)}^2 \\ &= \underbrace{-\rho \int_\Omega \partial_t \mathbf{u}_s \cdot \mathbf{v}^\epsilon (\chi - \Phi^\epsilon) - c_0 \int_\Omega \partial_t p_s \psi^\epsilon (\Phi^\epsilon - \chi) - \int_\Omega \boldsymbol{\sigma} (\nabla \mathbf{u}_s, \pi_s) : \nabla \mathbf{v}^\epsilon (\chi - \Phi^\epsilon)}_{I_1} \\ &\quad - \underbrace{\kappa \int_\Omega \nabla p_s \cdot \nabla \psi^\epsilon (\Phi^\epsilon - \chi) - \int_\Gamma p_s \mathbf{v}^\epsilon \cdot \mathbf{n} + \int_\Gamma \psi^\epsilon \mathbf{u}_s \cdot \mathbf{n} - \int_\Omega p_d^\epsilon \mathbf{v}^\epsilon \cdot \nabla \Phi^\epsilon + \int_\Omega \psi^\epsilon \mathbf{u}_d^\epsilon \cdot \nabla \Phi^\epsilon}_{I_2} \\ &\quad - \underbrace{\alpha_{BJ} \sum_{i=0}^{d-1} \left( \int_\Gamma (\mathbf{u}_s \cdot \boldsymbol{\tau}_i) (\mathbf{v}^\epsilon \cdot \boldsymbol{\tau}_i) - \int_\Omega (\mathbf{u}_d^\epsilon \cdot \tilde{\tau}_i) (\mathbf{v}^\epsilon \cdot \tilde{\tau}_i) |\nabla \Phi^\epsilon| \right)}_{I_3} + \underbrace{\int_\Omega (\mathbf{F} \cdot \mathbf{v}^\epsilon - g \psi^\epsilon) (\chi - \Phi^\epsilon)}_{I_4}. \end{aligned}$$

Here we used that  $\mathbf{u}_s$  and  $\mathbf{u}_d^\epsilon$  are divergence free, and therefore:

$$\int_\Omega \boldsymbol{\sigma} (\nabla (\mathbf{u}_s - \mathbf{u}_d^\epsilon), \pi_s - \pi_d^\epsilon) : \nabla (\mathbf{u}_s - \mathbf{u}_d^\epsilon) \Phi^\epsilon = 2\nu \int_\Omega |\mathbf{D}(\mathbf{u}_s - \mathbf{u}_d^\epsilon)|^2 \Phi^\epsilon.$$

Our goal is to estimate the right-hand side of (4.4) in terms of  $\epsilon$  and the norms of the sharp interface solution. This will be done by using the convergence results for the diffuse integrals from [18, Section 5],

and the following estimates which are consequences of the Poincaré's and Korn's inequalities for weighted spaces (Lemma 2.4 and [68, Thm 5.15]):

$$\|\mathbf{v}^\epsilon\|_{H^1(\Omega, \Phi^\epsilon)}^2 \lesssim \int_{\Omega} |\mathbf{D}(\mathbf{u}_s - \mathbf{u}_d^\epsilon)|^2 \Phi^\epsilon, \quad \|\psi^\epsilon\|_{H^1(\Omega, 1-\Phi^\epsilon)}^2 \lesssim \int_{\Omega} |\nabla(p_s - p_d^\epsilon)|^2 (1 - \Phi^\epsilon).$$

Here we used  $\|\mathbf{v}^\epsilon\|_{H^1(\Omega, \Phi^\epsilon)}^2 = \|\mathbf{v}^\epsilon\|_{H^1(\Omega_\epsilon, \Phi^\epsilon)}^2$  and  $\|\psi^\epsilon\|_{H^1(\Omega, 1-\Phi^\epsilon)}^2 = \|\psi^\epsilon\|_{H^1(\Omega \setminus \Omega_\epsilon, \Phi^\epsilon)}^2$ , where  $\Omega_\epsilon = \text{supp} \Phi^\epsilon$ . Therefore, we used the weighted Poincaré's and Korn's inequalities on  $\Omega^\epsilon$ .

The first integral is estimated by [18, Theorem 5.2] for  $p = 2$  as follows:

$$|I_1| \lesssim \epsilon^{3/2} (\rho \|\partial_t \mathbf{u}_s\|_{W^{1,\infty}} \|\mathbf{D}(\mathbf{u}_s - \mathbf{u}_d^\epsilon)\|_{L^2(\Omega, \Phi^\epsilon)} + c_0 \|\partial_t p_s\|_{W^{1,\infty}} \|\nabla(p_s - p_d^\epsilon)\|_{L^2(\Omega, 1-\Phi^\epsilon)}).$$

Similarly,

$$|I_6| \lesssim \epsilon^{3/2} (\|\mathbf{F}\|_{H^1(\Omega)} + \|g\|_{H^1(\Omega)}).$$

To evaluate  $I_2$ , we use the integration by parts:

$$\begin{aligned} I_2 &= \int_{\Omega} \nabla \cdot \boldsymbol{\sigma}(\nabla \mathbf{u}_s, \pi_s) \cdot \mathbf{v}^\epsilon (\chi - \Phi^\epsilon) - \int_{\Omega} \boldsymbol{\sigma}(\nabla \mathbf{u}_s, \pi_s) \nabla \Phi^\epsilon \cdot \mathbf{v}^\epsilon - \int_{\Gamma} \boldsymbol{\sigma}(\nabla \mathbf{u}_s, \pi_s) \mathbf{n} \cdot \mathbf{v}^\epsilon \\ &= \int_{\Omega} \nabla \cdot \boldsymbol{\sigma}(\nabla \mathbf{u}_s, \pi_s) \cdot \mathbf{v}^\epsilon (\chi - \Phi^\epsilon) - \int_{\Omega} \left( \boldsymbol{\sigma}(\nabla \mathbf{u}_s, \pi_s) \frac{\nabla \Phi^\epsilon}{|\nabla \Phi^\epsilon|} \cdot \frac{\nabla \Phi^\epsilon}{|\nabla \Phi^\epsilon|} \right) (\mathbf{v}^\epsilon \cdot \nabla \Phi^\epsilon) \\ &\quad - \sum_{i=1}^{d-1} \int_{\Omega} (\boldsymbol{\sigma}(\nabla \mathbf{u}_s, \pi_s) \tilde{\boldsymbol{\tau}}_i \cdot \tilde{\boldsymbol{\tau}}_i) (\mathbf{v}^\epsilon \cdot \tilde{\boldsymbol{\tau}}_i) |\nabla \Phi^\epsilon| + \int_{\Gamma} p_s \mathbf{v}^\epsilon \cdot \mathbf{n} + \alpha_{BJ} \sum_{i=1}^{d-1} \int_{\Gamma} (\mathbf{u}_s \cdot \boldsymbol{\tau}_i) (\mathbf{v}^\epsilon \cdot \boldsymbol{\tau}_i), \end{aligned}$$

In a similar way, we have:

$$I_3 = \kappa \int_{\Omega} \Delta p_s \psi^\epsilon (\chi - \Phi^\epsilon) + \kappa \int_{\Omega} \psi^\epsilon \nabla p_s \cdot \nabla \Phi^\epsilon + \int_{\Gamma} \psi^\epsilon \underbrace{\kappa \nabla p_s \cdot \mathbf{n}}_{-\mathbf{u}_s \cdot \mathbf{n}},$$

and

$$\begin{aligned} I_4 &= \underbrace{\int_{\Omega} (p_s - p_d^\epsilon) \mathbf{v}^\epsilon \cdot \nabla \Phi^\epsilon - \int_{\Omega} \psi^\epsilon (\mathbf{u}_s - \mathbf{u}_d^\epsilon) \cdot \nabla \Phi^\epsilon}_0 \\ &\quad - \int_{\Omega} p_s \mathbf{v}^\epsilon \cdot \nabla \Phi^\epsilon - \int_{\Gamma} p_s \mathbf{v}^\epsilon \cdot \mathbf{n} + \int_{\Omega} \psi^\epsilon \mathbf{u}_s \cdot \nabla \Phi^\epsilon + \int_{\Gamma} \psi^\epsilon \mathbf{u}_s \cdot \mathbf{n}, \end{aligned}$$

and

$$I_5 = -\alpha_{BJ} \sum_{i=1}^{d-1} \int_{\Omega} |(\mathbf{u}_s - \mathbf{u}_d^\epsilon) \cdot \tilde{\boldsymbol{\tau}}_i|^2 |\nabla \Phi^\epsilon| + \alpha_{BJ} \sum_{i=1}^{d-1} \int_{\Omega} (\mathbf{u}_s \cdot \tilde{\boldsymbol{\tau}}_i) (\mathbf{v}^\epsilon \cdot \tilde{\boldsymbol{\tau}}_i) |\nabla \Phi^\epsilon| - \alpha_{BJ} \sum_{i=1}^{d-1} \int_{\Gamma} (\mathbf{u}_s \cdot \boldsymbol{\tau}_i) (\mathbf{v}^\epsilon \cdot \boldsymbol{\tau}_i).$$

Adding the estimates for  $I_2, I_3, I_4$  and  $I_5$  together, we obtain:

$$\begin{aligned} I_2 + I_3 + I_4 + I_5 &= -\alpha_{BJ} \sum_{i=1}^{d-1} \int_{\Omega} |(\mathbf{u}_s - \mathbf{u}_d^\epsilon) \cdot \tilde{\boldsymbol{\tau}}_i|^2 |\nabla \Phi^\epsilon| + \int_{\Omega} (\nabla \cdot \boldsymbol{\sigma}(\nabla \mathbf{u}_s, \pi_s) \cdot \mathbf{v}^\epsilon + \kappa \Delta p_s \psi^\epsilon) (\chi - \Phi^\epsilon) \\ &\quad + \int_{\Omega} \psi^\epsilon (\mathbf{u}_s + \kappa \nabla p_s) \cdot \nabla \Phi^\epsilon + \int_{\Omega} \left( -p_s - \boldsymbol{\sigma}(\nabla \mathbf{u}_s, \pi_s) \frac{\nabla \Phi^\epsilon}{|\nabla \Phi^\epsilon|} \cdot \frac{\nabla \Phi^\epsilon}{|\nabla \Phi^\epsilon|} \right) (\mathbf{v}^\epsilon \cdot \nabla \Phi^\epsilon) \\ &\quad + \sum_{i=1}^{d-1} \int_{\Omega} (\alpha_{BJ} \mathbf{u}_s \cdot \tilde{\boldsymbol{\tau}}_i - \boldsymbol{\sigma}(\nabla \mathbf{u}_s, \pi_s) \tilde{\boldsymbol{\tau}}_i \cdot \tilde{\boldsymbol{\tau}}_i) (\mathbf{v}^\epsilon \cdot \tilde{\boldsymbol{\tau}}_i) |\nabla \Phi^\epsilon|. \end{aligned}$$

The first term has a negative sign and will be combined with the terms on the left-hand side. The second term can be again estimated by [18, Theorem 5.2]:

$$\begin{aligned} & \left| \int_{\Omega} (\nabla \cdot \boldsymbol{\sigma}(\nabla \mathbf{u}_s, \pi_s) \cdot \mathbf{v}^\epsilon + \kappa \Delta p_s \psi^\epsilon) (\chi - \Phi^\epsilon) \right| \\ & \lesssim \epsilon^{3/2} (\|\nabla \cdot \boldsymbol{\sigma}(\nabla \mathbf{u}_s, \pi_s)\|_{W^{1,\infty}} \|\mathbf{D}(\mathbf{u}_s - \mathbf{u}_d^\epsilon)\|_{L^2(\Omega, \Phi^\epsilon)} + \|\Delta p_s\|_{W^{1,\infty}} \|\nabla(p_s - p_d^\epsilon)\|_{L^2(\Omega, 1 - \Phi^\epsilon)}). \end{aligned}$$

To estimate the last three terms first we notice that in the tubular neighborhood of  $\Gamma$  we have  $\mathbf{n} = -\frac{\nabla \Phi^\epsilon}{|\nabla \Phi^\epsilon|}$  and  $\boldsymbol{\tau}_i = -\tilde{\boldsymbol{\tau}}_i, i = 1, 2, \dots, d-1$ . Therefore, using the coupling conditions, the following equalities hold on  $\Gamma$ :

$$\begin{aligned} (\mathbf{u}_s + \kappa \nabla p_s) \cdot \nabla \Phi^\epsilon &= 0, \quad \left( -p_s - \boldsymbol{\sigma}(\nabla \mathbf{u}_s, \pi_s) \frac{\nabla \Phi^\epsilon}{|\nabla \Phi^\epsilon|} \cdot \frac{\nabla \Phi^\epsilon}{|\nabla \Phi^\epsilon|} \right) = 0, \\ (\alpha_{BJ} \mathbf{u}_s \cdot \tilde{\boldsymbol{\tau}}_i - \boldsymbol{\sigma}(\nabla \mathbf{u}_s, \pi_s) \tilde{\boldsymbol{\tau}}_i \cdot \tilde{\boldsymbol{\tau}}_i) &= 0. \end{aligned}$$

Hence, we can use [18, Theorem 5.6] to bound the last three terms by:

$$C\epsilon^{3/2} (\|\mathbf{u}_s\|_{H^3(\Omega)} + \|\pi_s\|_{H^2(\Omega)} + \|p_s\|_{H^3(\Omega)}) (\|\mathbf{D}(\mathbf{u}_s - \mathbf{u}_d^\epsilon)\|_{L^2(\Omega, \Phi^\epsilon)} + \|\nabla(p_s - p_d^\epsilon)\|_{L^2(\Omega, 1 - \Phi^\epsilon)}).$$

Combining all the obtained estimates and using Young's inequality, we get the following error estimate:

$$\begin{aligned} & \frac{1}{2} \frac{d}{dt} \left( \rho \|\mathbf{u}_s - \mathbf{u}_d^\epsilon\|_{L^2(\Omega, \Phi^\epsilon)}^2 + c_0 \|p_s - p_d^\epsilon\|_{L^2(\Omega, 1 - \Phi^\epsilon)}^2 \right) + \nu \|\mathbf{D}(\mathbf{u}_s - \mathbf{u}_d^\epsilon)\|_{L^2(\Omega, \Phi^\epsilon)} + \frac{\kappa}{2} \|\nabla(p_s - p_d^\epsilon)\|_{L^2(\Omega, 1 - \Phi^\epsilon)} \\ & \quad + \alpha_{BJ} \sum_{i=1}^{d-1} \int_{\Omega} |(\mathbf{u}_s - \mathbf{u}_d^\epsilon) \cdot \tilde{\boldsymbol{\tau}}_i|^2 |\nabla \Phi^\epsilon| \\ & \lesssim \epsilon^3 (\|\partial_t \mathbf{u}_s\|_{W^{1,\infty}}^2 + \|\partial_t p_s\|_{W^{1,\infty}}^2 + \|\mathbf{u}_s\|_{W^{3,\infty}}^2 + \|\pi_s\|_{W^{2,\infty}}^2 + \|p_s\|_{W^{3,\infty}}^2 + \|\mathbf{F}\|_{H^1} + \|g\|_{H^1}). \end{aligned}$$

The final result (4.3) is obtained by integrating the estimate above from 0 to  $t$ .  $\square$

**5. Numerical results.** Using the numerical simulations, we investigate the accuracy of the diffuse interface method. For this purpose, we use a method of manufactured solutions on a benchmark problem previously used in [5]. We define the Stokes domain as  $\Omega_F = (0, 1) \times (0, 1)$  and the Darcy domain as  $\Omega_D = (0, 1) \times (1, 2)$ . Therefore, the computational domain used in this example is  $\Omega = \Omega_F \cup \Omega_D = (0, 1) \times (0, 2)$ . The phase field function is defined as

$$\Phi^\epsilon = \frac{1}{2} \left( 1 + \tanh \left( \frac{y-1}{\epsilon} \right) \right),$$

and regularized as in (2.4).

We assume that the exact solution is given by

$$\begin{aligned} \begin{bmatrix} u_x^{exact} \\ u_y^{exact} \end{bmatrix} &= \begin{bmatrix} -\frac{1}{\hat{\pi}} e^y \sin(\hat{\pi}x) \cos(2\hat{\pi}t) \\ (e^y - e) \cos(\hat{\pi}x) \cos(2\hat{\pi}t) \end{bmatrix}, \\ \pi^{exact} &= 2e^y \cos(\hat{\pi}x) \cos(2\hat{\pi}t), \\ p^{exact} &= (e^y - ey) \cos(\hat{\pi}x) \cos(2\hat{\pi}t), \end{aligned}$$

where  $\pi^{exact}$  denotes the exact Stokes pressure, and  $\hat{\pi}$  denotes the constant approximately equal to 3.14159. Using the exact solution, we compute the external forces  $g$  and  $\mathbf{F}$  that appear on the right-hand side in (2.3) and (2.1), respectively. On the bottom boundary, we impose the Dirichlet condition for the Darcy pressure, and on the top boundary we impose the Dirichlet condition for the Stokes velocity. On the left and right boundaries, we impose the Neumann conditions for both Stokes and Darcy regions. All the boundary conditions are computed using the exact solution. We note that the Neumann conditions are imposed using the diffuse interface approach as follows:

$$\int_{\Gamma_{\text{left/right}}^F} \boldsymbol{\sigma} \mathbf{n} \cdot \mathbf{v} = \int_{\Gamma_{\text{left/right}}} \boldsymbol{\sigma} \mathbf{n} \cdot \mathbf{v} \Phi^\epsilon,$$

$$\int_{\Gamma_{\text{left/right}}^D} \boldsymbol{\kappa} \nabla p \mathbf{n} \psi = \int_{\Gamma_{\text{left/right}}} \boldsymbol{\kappa} \nabla p \mathbf{n} \psi (1 - \Phi^\epsilon),$$

where  $\Gamma_{\text{left/right}}^F$  and  $\Gamma_{\text{left/right}}^D$  denote the left and right boundaries to  $\Omega_F$  and  $\Omega_D$ , respectively, and  $\Gamma_{\text{left/right}}$  denotes the left and right boundary to  $\Omega$ .

In this example, all the parameters are set to one, i.e.,  $\rho = \nu = c_0 = \alpha_{BJ} = 1$  and  $\boldsymbol{\kappa} = \mathbb{I}$ , where  $\mathbb{I}$  is the identity matrix. The final time used in this example is  $T = 1$ . To compute the rates of convergence, we choose initial  $\Delta t = h = 1/5$  and then refine the spatial and the temporal meshes by dividing the parameters by 2. We use  $\mathbb{P}_2 - \mathbb{P}_1$  elements for the Stokes velocity and pressure, and  $\mathbb{P}_2$  elements for the Darcy pressure. The finite element solver *FreeFem++* [69] is used for computations. The value of  $\epsilon$  depends on the mesh size and is defined as  $\epsilon = h$ . We initially set  $\delta = 10^{-3}$ , and then refine by dividing by 2 at the same rate as the spatial and temporal parameters. We define the total pressure and velocity, and the relative errors in the following way:

$$\begin{aligned} \mathbf{u}_{tot} &= \mathbf{u} \Phi^\epsilon + \mathbf{q} (1 - \Phi^\epsilon), & \mathbf{e}_u &= \frac{\|\mathbf{u}_{tot}^{exact} - \mathbf{u}_{tot}^\epsilon\|_{L^2(\Omega)}}{\|\mathbf{u}_{tot}^{exact}\|_{L^2(\Omega)}}, \\ p_{tot} &= \pi \Phi^\epsilon + p (1 - \Phi^\epsilon), & e_p &= \frac{\|\pi_{tot}^{exact} - \pi_{tot}^\epsilon\|_{L^2(\Omega)}}{\|\pi_{tot}^{exact}\|_{L^2(\Omega)}}. \end{aligned}$$

The errors and the rates of convergence are given in Table 1. We also plot the Darcy pressure and the fluid

$h$	$\mathbf{e}_u$	rate	$e_p$	rate
1/5	$1.568 \cdot 10^{-1}$	-	$2.197 \cdot 10^{-1}$	-
1/10	$8.850 \cdot 10^{-3}$	4.15	$1.224 \cdot 10^{-2}$	4.17
1/20	$1.647 \cdot 10^{-3}$	2.43	$2.303 \cdot 10^{-3}$	2.41
1/40	$3.483 \cdot 10^{-4}$	2.24	$5.164 \cdot 10^{-4}$	2.16
1/80	$7.859 \cdot 10^{-5}$	2.15	$1.228 \cdot 10^{-4}$	2.07

Table 1: Rates of convergence for the total velocity and pressure obtained with  $\Delta t = h$ ,  $\epsilon = h$ , and  $\mathbb{P}_2 - \mathbb{P}_1$  elements for the Stokes velocity and pressure and  $\mathbb{P}_1$  elements for the Darcy pressure. The regularization parameter,  $\delta$ , is initially set to  $10^{-3}$ , and then refined at the same rate as  $\Delta t$  and  $h$ .

velocity over the interface  $\Gamma = (0, 1) \times \{1\}$ . Figure 1 shows the total pressure (left) and the magnitude of the total velocity (right) obtained for different values of  $h$ . We observe that the approximated solutions converge towards the exact ones as  $h$  decreases. We note that the uniform meshes are used in this example. A more accurate approximation can be obtained if the meshes are refined near the interface, see for example [31]. However, the rates of convergence should not be affected.



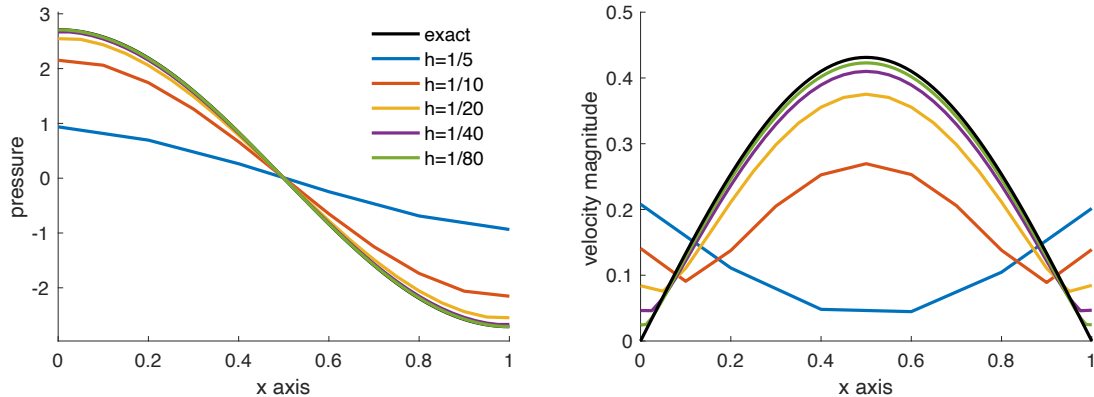


Fig. 1: The total pressure (left) and the total velocity magnitude (right) over the interface  $\Gamma = (0, 1) \times \{1\}$  obtained for different values of  $h$ .

**6. Conclusions.** In this work, we considered the time dependent Stokes-Darcy coupled problem formulated using a diffuse interface approach. The focus of the paper is the analysis of the convergence of the diffuse interface formulation to the sharp interface form. We performed the analysis by studying separately the modeling error resulting from the difference between the sharp and diffuse interface formulations at the continuous level, and the approximation error obtained when analyzing the difference between the continuous and discrete diffuse interface formulations. We analyzed the approximation error assuming that the phase-field function is regularized, as described in (2.4), where  $\delta$  was assumed to be a fixed positive number. The convergence is also obtained if  $\delta \rightarrow 0$  and  $\Delta t$  and  $h$  are assumed to be proportional to the powers of  $\delta$ . In the analysis of the modeling error, we assumed that  $\delta = 0$ , obtaining a modeling error of order  $\mathcal{O}(\epsilon^{\frac{3}{2}})$ . We computed the numerical rates of convergence, where we assumed that  $\Delta t, h, \epsilon$  and  $\delta$  all decrease at the same rate. Even though the error estimates depend on the powers of  $\delta^{-1}$  and the modeling error is  $\mathcal{O}(\epsilon^{\frac{3}{2}})$  (similar as in [18]), higher order convergence rates were obtained numerically. Our future work will focus on the analysis of the problem when  $\delta = 0$ , which relies on the theory of weighted spaces with Muckenhoupt weights.

#### REFERENCES

- [1] G. Du, Q. Li, and Y. Zhang, *A two-grid method with backtracking for the mixed Navier–Stokes/Darcy model*, Numerical Methods for Partial Differential Equations **36** (2020), 1601–1610.
- [2] V. Girault, D. Vassilev, and I. Yotov, *Mortar multiscale finite element methods for Stokes–Darcy flows*, Numerische Mathematik **127** (2014), 93–165.
- [3] E. Burman and P. Hansbo, *A unified stabilized method for Stokes’ and Darcy’s equations*, Journal of Computational and Applied Mathematics **198** (2007), 35–51.
- [4] J. Yu, Y. Sun, F. Shi, and H. Zheng, *Nitsche’s type stabilized finite element method for the fully mixed Stokes–Darcy problem with Beavers–Joseph conditions*, Applied Mathematics Letters **110** (2020), 106588.
- [5] W. Layton, H. Tran, and X. Xiong, *Long time stability of four methods for splitting the evolutionary Stokes–Darcy problem into Stokes and Darcy subproblems*, Journal of Computational and Applied Mathematics **236** (2012), 3198–3217.
- [6] M. Kubacki and M. Moraiti, *Analysis of a second-order, unconditionally stable, partitioned method for the evolutionary Stokes–Darcy model*, International Journal of Numerical Analysis & Modeling **12** (2015), 704–730.
- [7] W. Layton, H. Tran, and C. Trenchea, *Analysis of long time stability and errors of two partitioned methods for uncoupling evolutionary groundwater–surface water flows*, SIAM Journal on Numerical Analysis **51** (2013), 248–272.
- [8] W. Layton and C. Trenchea, *Stability of two IMEX methods, CNLF and BDF2-AB2, for uncoupling systems of evolution equations*, Applied Numerical Mathematics **62** (2012), 112–120.
- [9] W. Chen, M. Gunzburger, D. Sun, and X. Wang, *Efficient and long-time accurate second-order methods for the Stokes–Darcy system*, SIAM Journal on Numerical Analysis **51** (2013), 2563–2584.
- [10] M. Gunzburger, X. He, and B. Li, *On Stokes–Ritz projection and multistep backward differentiation schemes in decoupling the Stokes–Darcy model*, SIAM Journal on Numerical Analysis **56** (2018), 397–427.
- [11] W. Chen, M. Gunzburger, D. Sun, and X. Wang, *An efficient and long-time accurate third-order algorithm for the Stokes–Darcy system*, Numerische Mathematik **134** (2016), 857–879.

- [12] M. Discacciati, A. Quarteroni, and A. Valli, *Robin–Robin domain decomposition methods for the Stokes–Darcy coupling*, SIAM Journal on Numerical Analysis **45** (2007), 1246–1268.
- [13] M. Discacciati and L. Gerardo-Giorda, *Optimized Schwarz methods for the Stokes–Darcy coupling*, IMA Journal of Numerical Analysis **38** (2018), 1959–1983.
- [14] A. Bueno-Orovio, V. M. Perez-Garcia, and F. H. Fenton, *Spectral methods for partial differential equations in irregular domains: the spectral smoothed boundary method*, SIAM Journal on Scientific Computing **28** (2006), 886–900.
- [15] A. Rätz and A. Voigt, *PDE’s on surfaces—a diffuse interface approach*, Communications in Mathematical Sciences **4** (2006), 575–590.
- [16] X. Li, J. Lowengrub, A. Rätz, and Voigt, *Solving PDEs in complex geometries: a diffuse domain approach*, Communications in Mathematical Sciences **7** (2009), 81–107.
- [17] K. Lervag and J. Lowengrub, *Analysis of the diffuse-domain method for solving PDEs in complex geometries*, Communications in Mathematical Sciences **13** (2015), 1473–1500.
- [18] M. Burger, O. L. Elvetun, and M. Schlottbom, *Analysis of the diffuse domain method for second order elliptic boundary value problems*, Foundations of Computational Mathematics **17** (2017), 627–674.
- [19] D. M. Anderson, G. B. McFadden, and A. A. Wheeler, *Diffuse-interface methods in fluid mechanics*, Annual Review of Fluid Mechanics **30** (1998), 139–165.
- [20] Q. Du and X. Feng, *The phase field method for geometric moving interfaces and their numerical approximations*, Handbook of Numerical Analysis **21** (2020), 425–508.
- [21] Y. G. Chen, Y. Giga, and S. Goto, *Uniqueness and existence of viscosity solutions of generalized mean curvature flow equations*, Journal of Differential Geometry **33** (1991), 749–786.
- [22] S. Osher and J. A. Sethian, *Fronts propagating with curvature-dependent speed: Algorithms based on Hamilton–Jacobi formulations*, Journal of Computational Physics **79** (1988), 12–49.
- [23] S. Osher and R. P. Fedkiw, *Level set methods and dynamic implicit surfaces*, Vol. 153, Springer, 2003.
- [24] G. Pacquaut, J. Bruchon, N. Moulin, and S. Drapier, *Combining a level-set method and a mixed stabilized P1/P1 formulation for coupling Stokes–Darcy flows*, International Journal for Numerical Methods in Fluids **69** (2012), 459–480.
- [25] I. Ramiere, P. Angot, and M. Belliard, *A fictitious domain approach with spread interface for elliptic problems with general boundary conditions*, Computer Methods in Applied Mechanics and Engineering **196** (2007), 766–781.
- [26] I. Ramière, P. Angot, and M. Belliard, *A general fictitious domain method with immersed jumps and multilevel nested structured meshes*, Journal of Computational Physics **225** (2007), 1347–1387.
- [27] C. S. Peskin, *The immersed boundary method*, Acta Numerica **11** (2002), 479–517.
- [28] B. E. Griffith and C. S. Peskin, *On the order of accuracy of the immersed boundary method: Higher order convergence rates for sufficiently smooth problems*, Journal of Computational Physics **208** (2005), 75–105.
- [29] B. Maury, *A fat boundary method for the Poisson problem in a domain with holes*, Journal of Scientific Computing **16** (2001), 319–339.
- [30] S. Bertoluzza, M. Ismail, and B. Maury, *Analysis of the fully discrete fat boundary method*, Numerische Mathematik **118** (2011), 49–77.
- [31] S. K. Stoter, P. Müller, L. Cicalese, M. Tuveri, D. Schillinger, and T. J. Hughes, *A diffuse interface method for the Navier–Stokes/Darcy equations: Perfusion profile for a patient-specific human liver based on MRI scans*, Computer Methods in Applied Mechanics and Engineering **321** (2017), 70–102.
- [32] K. E. Teigen, X. Li, J. Lowengrub, F. Wang, and A. Voigt, *A diffuse-interface approach for modeling transport, diffusion and adsorption/desorption of material quantities on a deformable interface*, Communications in Mathematical Sciences **4** (2009), 1009.
- [33] C. M. Elliott, B. Stinner, V. Styles, and R. Welford, *Numerical computation of advection and diffusion on evolving diffuse interfaces*, IMA Journal of Numerical Analysis **31** (2011), 786–812.
- [34] S. Aland, J. Lowengrub, and A. Voigt, *Two-phase flow in complex geometries: A diffuse domain approach*, Computer Modeling in Engineering & Sciences **57** (2010), 77.
- [35] K. E. Teigen, P. Song, J. Lowengrub, and A. Voigt, *A diffuse-interface method for two-phase flows with soluble surfactants*, Journal of Computational Physics **230** (2011), 375–393.
- [36] C. Miehe, M. Hofacker, and F. Welschinger, *A phase field model for rate-independent crack propagation: Robust algorithmic implementation based on operator splits*, Computer Methods in Applied Mechanics and Engineering **199** (2010), 2765–2778.
- [37] M. J. Borden, C. V. Verhoosel, M. A. Scott, T. J. Hughes, and C. M. Landis, *A phase-field description of dynamic brittle fracture*, Computer Methods in Applied Mechanics and Engineering **217** (2012), 77–95.
- [38] A. Mikelic, M. F. Wheeler, and T. Wick, *A phase-field method for propagating fluid-filled fractures coupled to a surrounding porous medium*, Multiscale Modeling & Simulation **13** (2015), 367–398.
- [39] H. Gomez, L. Cueto-Felgueroso, and R. Juanes, *Three-dimensional simulation of unstable gravity-driven infiltration of water into a porous medium*, Journal of Computational Physics **238** (2013), 217–239.
- [40] J. Liu, C. M. Landis, H. Gomez, and T. J. Hughes, *Liquid–vapor phase transition: Thermomechanical theory, entropy stable numerical formulation, and boiling simulations*, Computer Methods in Applied Mechanics and Engineering **297** (2015), 476–553.
- [41] D. M. Saylor, C. Forrey, C.-S. Kim, and J. A. Warren, *Diffuse interface methods for modeling drug-eluting stent coatings*, Annals of Biomedical Engineering **44** (2016), 548–559.
- [42] M. Burger, O. L. Elvetun, and M. Schlottbom, *Diffuse interface methods for inverse problems: case study for an elliptic Cauchy problem*, Inverse Problems **31** (2015), 125002.
- [43] M. Schlottbom, *Error analysis of a diffuse interface method for elliptic problems with Dirichlet boundary conditions*,

- Applied Numerical Mathematics **109** (2016), 109–122.
- [44] S. Franz, H.-G. Roos, R. Gärtner, and A. Voigt, *A note on the convergence analysis of a diffuse-domain approach*, Computational Methods in Applied Mathematics **12** (2012), 153–167.
- [45] L. H. Nguyen, S. K. Stoter, M. Ruess, M. A. Sanchez Uribe, and D. Schilling, *The diffuse Nitsche method: Dirichlet constraints on phase-field boundaries*, International Journal for Numerical Methods in Engineering **113** (2018), 601–633.
- [46] H. Abels and S. Schaubek, *Sharp interface limit for the Cahn–Larché system*, Asymptotic Analysis **91** (2015), 283–340.
- [47] Y. Gao, X. He, L. Mei, and X. Yang, *Decoupled, linear, and energy stable finite element method for the Cahn–Hilliard–Navier–Stokes–Darcy phase field model*, SIAM Journal on Scientific Computing **40** (2018), B110–B137.
- [48] H. Abels, *On a diffuse interface model for two-phase flows of viscous, incompressible fluids with matched densities*, Archive for Rational Mechanics and Analysis **194** (2009), 463–506.
- [49] H. Abels and D. Lengeler, *On sharp interface limits for diffuse interface models for two-phase flows*, Interfaces and Free Boundaries **16** (2014), 395–418.
- [50] E. Feireisl, H. Petzeltová, E. Rocca, and G. Schimperna, *Analysis of a phase-field model for two-phase compressible fluids*, Mathematical Models and Methods in Applied Sciences **20** (2010), 1129–1160.
- [51] H. Abels, Y. Liu, and A. Schöttl, *Sharp interface limits for diffuse interface models for two-phase flows of viscous incompressible fluids*, in Transport Processes at Fluidic Interfaces, Springer, 2017, pp. 231–253.
- [52] Z. Guo, F. Yu, P. Lin, S. Wise, and J. Lowengrub, *A diffuse domain method for two-phase flows with large density ratio in complex geometries*, Journal of Fluid Mechanics **907** (2021), A38.
- [53] D. Ray, C. Liu, and B. Riviere, *A discontinuous Galerkin method for a diffuse-interface model of immiscible two-phase flows with soluble surfactant*, Computational Geosciences **25** (2021), 1775–1792.
- [54] J. Yang, S. Mao, X. He, X. Yang, and Y. He, *A diffuse interface model and semi-implicit energy stable finite element method for two-phase magnetohydrodynamic flows*, Computer Methods in Applied Mechanics and Engineering **356** (2019), 435–464.
- [55] H. Abels and Y. Liu, *Sharp interface limit for a Stokes/Allen–Cahn system*, Archive for Rational Mechanics and Analysis **229** (2018), 417–502.
- [56] M. Discacciati, E. Miglio, and A. Quarteroni, *Mathematical and numerical models for coupling surface and groundwater flows*, Applied Numerical Mathematics **43** (2002), 57–74.
- [57] Y. Cao, M. Gunzburger, F. Hua, X. Wang, et al., *Coupled Stokes–Darcy model with Beavers–Joseph interface boundary condition*, Communications in Mathematical Sciences **8** (2010), 1–25.
- [58] W. Martin, E. Cohen, R. Fish, and P. Shirley, *Practical ray tracing of trimmed nurbs surfaces*, Journal of Graphics Tools **5** (2000), 27–52.
- [59] R. H. Nochetto, E. Otárola, and A. J. Salgado, *Piecewise polynomial interpolation in Muckenhoupt weighted Sobolev spaces and applications*, Numerische Mathematik **132** (2016), 85–130.
- [60] M. Discacciati and A. Quarteroni, *Navier–Stokes/Darcy coupling: modeling, analysis, and numerical approximation*, Revista Matemática Complutense **22** (2009), 315–426.
- [61] G. P. Galdi, *An introduction to the mathematical theory of the Navier–Stokes equations*, Springer Monographs in Mathematics, second edition, Springer, New York, 2011 (Steady-state problems).
- [62] R. Temam, *Navier–Stokes equations*, Vol. 2 of *Studies in Mathematics and its Applications*, Revised edition, North-Holland Publishing Co., Amsterdam–New York, 1979 (Theory and numerical analysis, With an appendix by F. Thomasset).
- [63] V. Girault and P.-A. Raviart, *Finite element approximation of the Navier–Stokes equations*, LNM **749**.
- [64] Z. Luo, *Mixed finite element methods and applications*, Chinese Science Press, Beijing, 2006.
- [65] R. H. Nochetto, E. Otárola, and A. J. Salgado, *Piecewise polynomial interpolation in Muckenhoupt weighted Sobolev spaces and applications*, Numerische Mathematik **132** (2016), 85–130.
- [66] A. Kalamajska, *Coercive inequalities on weighted Sobolev spaces*, Colloquium Mathematicum **66** (1994), 309–318.
- [67] K. Schumacher, *Solutions to the equation  $\operatorname{div} u = f$  in weighted Sobolev spaces*, in Parabolic and Navier–Stokes equations. Part 2, Vol. 81 of *Banach Center Publications*, Institute of Mathematics of the Polish Academy of Sciences, 2008, pp. 433–440.
- [68] L. Diening, M. Ruzička, and K. Schumacher, *A decomposition technique for John domains*, Annales Academiæ Scientiarum Fennicæ. Mathematica **35** (2010), 87–114.
- [69] F. Hecht, *New development in FreeFem++*, Journal of Numerical Mathematics **20** (2012), 251–266.